AD-A069 909   SYRACUSE UNIV N Y DEPT OF CHEMICAL ENGINEERING AND --ETC F/G 11/6
EXPLORATORY STUDY OF THE DYNAMIC FRACTURE DUCTILITY OF TRIP AND--ETC(U)
FEB 79 V WEISS, A WU, J BIEGEL   DAAG46-77-C-0019
UNCLASSIFIED   AMMRO-TR-79-8   NL

| OF |
AD
A069909

END
DATE
FILMED
7-79
DDC

AD

ARMY MATERIALS AND MECHANICS RESEARCH CENTER

AMMRC TR 79-8

EXPLORATORY STUDY OF THE DYNAMIC FRACTURE DUCTILITY OF TRIP AND 300M STEELS

FEBRUARY 1979

Department of Chemical Engineering and Materials Science
409 Link Hall, Syracuse, New York 13210

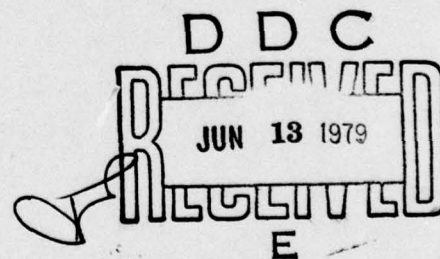FINAL REPORT   CONTRACT NUMBER   DAAG46-77-C-0019

DDC
RECEIVED
JUN 13 1979
E

Prepared for

ARMY MATERIALS AND MECHANICS RESEARCH CENTER
Watertown, Massachusetts 02172

79 06 11 055

The findings in this report are not to be construed as an official Department of the Army position, unless so designated by other authorized documents.

Mention of any trade names or manufacturers in this report shall not be construed as advertising nor as an official indorsement or approval of such products or companies by the United States Government.

REPORT DOCUMENTATION PAGE		READ INSTRUCTIONS BEFORE COMPLETING FORM
1. REPORT NUMBER AMMRC TR-79-8	2. GOVT ACCESSION NO.	3. RECIPIENT'S CATALOG NUMBER
4. TITLE (and Subtitle) Exploratory Study of the Dynamic Fracture Ductility of TRIP and 300M Steels		5. TYPE OF REPORT & PERIOD COVERED Final Report
		6. PERFORMING ORG. REPORT NUMBER
7. AUTHOR(s) Volker Weiss Albert Wu John Biegel		8. CONTRACT OR GRANT NUMBER(s) DAAG46-77-C-0019
9. PERFORMING ORGANIZATION NAME AND ADDRESS		10. PROGRAM ELEMENT, PROJECT, TASK AREA & WORK UNIT NUMBERS D/A Project: 1L162105AH84
11. CONTROLLING OFFICE NAME AND ADDRESS Army Materials and Mechanics Research Center Watertown, Massachusetts 02172		12. REPORT DATE February, 1979
		13. NUMBER OF PAGES
14. MONITORING AGENCY NAME & ADDRESS(if different from Controlling Office)		15. SECURITY CLASS. (of this report) Unclassified
		15a. DECLASSIFICATION/DOWNGRADING SCHEDULE

16. DISTRIBUTION STATEMENT (of this Report)

Approved for public release; distribution unlimited.

17. DISTRIBUTION STATEMENT (of the abstract entered in Block 20, if different from Report)

18. SUPPLEMENTARY NOTES

19. KEY WORDS (Continue on reverse side if necessary and identify by block number)

TRIP steels	Mechanical properties	Fracture
300M steels	Dynamic properties	
High strength steels	Transformation plasticity	

20. ABSTRACT (Continue on reverse side if necessary and identify by block number)

The bulge characteristics of 300M steel and TRIP steel were studied at various strain rates and stress states. The 300M steel was heat-treated to two conditions; isothermally transformed, and normalized. The TRIP steel was processed to four conditions by means of various amounts of warm working. The inherent directionality of TRIP steel required the development of a biaxial test for various strain rates other than the equibiaxial bulge test where the stress ratio, $\alpha = \sigma_2/\sigma_1$, is not equal to 1. Two testing methods were developed:

DD FORM 1473 EDITION OF 1 NOV 65 IS OBSOLETE
1 JAN 73

Block No. 20

1) a bulge test through an elliptical die, which gives a stress state of $\alpha = 0.9$, and 2) a plane strain tensile test, which gives a stress state of $\alpha = 1/2$.

The basic mechanical properties of the materials are given through their true stress-true strain curves. The equibiaxial bulge tests at three strain rates ($\dot{\varepsilon} \simeq 10^{-4}$ sec^{-1}, 10^{-1} sec^{-1}, 10^{3} sec^{-1}) on the isothermally transformed 300M steel show that the fracture ductility increases with increasing strain rate. On the basis of the reported correlation between a true effective fracture strain from a bulge test and the plane strain fracture toughness, a similar increase in fracture toughness with increasing strain rate is expected. At low strain rate the fracture ductility of TRIP steel is a function of the stress state at fracture and of the amount of warm-work during TRIP processing. The minimum value of the fracture ductility of TRIP steel at low strain rates is observed for a stress state $\alpha = 1$, which is in agreement with previous results on high strength steel and the critical mean stress fracture criterion proposed by Weiss. For the two high strength TRIP steels (79% warm-work and 30% warm-work), the plane strain fracture ductility decreases with increasing strain rate. A similar decrease of the plane strain fracture toughness with increasing strain rate is expected. Adiabatic heating and consequent repression of the martensite formation is suggested as the principal responsible mechanism.

Accession For

NTIS GRA&I	X
DDC TAB	
Unannounced	
Justification	

By

Distribution/

Availability Codes

Dist	Avail and/or special
A	

FOREWORD

This report contains the findings of a research program entitled "Exploratory Study of the Dynamic Fracture Ductility of TRIP and 300M Steels" under contract number DAAG46-77-C-0019 with Dr. M. Azrin of Army Materials and Mechanics Research Center serving as Contracting Officer. The study was conducted in Syracuse University's Department of Cnemical Engineering and Materials Science under the direction of Dr. Volker Weiss, Professor of Materials Science.

EXPLORATORY STUDY OF THE DYNAMIC FRACTURE DUCTILITY OF TRIP AND 300M STEELS

ABSTRACT

The bulge characteristics of 300M steel and TRIP steel were studied at various strain rates and stress states. The 300M steel was heat-treated to two conditions; isothermally transformed, and normalized. The TRIP steel was processed to four conditions by means of various amounts of warm working. The inherent directionality of TRIP steel required the development of a biaxial test for various strain rates other than the equibiaxial bulge test where the stress ratio, $\alpha = \sigma_2/\sigma_1$, is not equal to 1. Two testing methods were developed: 1) a bulge test through an elliptical die, which gives a stress state of $\alpha = 0.9$, and 2) a plane strain tensile test, which gives a stress state of $\alpha = 1/2$.

The basic mechanical properties of the materials are given through their true stress-true strain curves. The equibiaxial bulge tests at three strain rates ($\dot{\varepsilon} \approx 10^{-4}$ sec^{-1}, 10^{-1} sec^{-1}, 10^3 sec^{-1}) on the isothermally transformed 300M steel show that the fracture ductility increases with increasing strain rate. On the basis of the reported correlation between a true effective fracture strain from a bulge test and the plane strain fracture toughness, a similar increase in fracture toughness with increasing strain rate is expected. At low strain rate the fracture ductility of TRIP steel is a function of the stress state at fracture and of the amount of warm-work during TRIP processing. The minimum value of the fracture ductility of TRIP steel at low strain rates is observed for a stress state $\alpha = 1$, which is in agreement with previous results on high strength steel and the critical mean stress fracture criterion proposed by Weiss. For the two high strength TRIP steels (79% warm-work and 30% warm-work), the plane strain fracture ductility decreases with increasing strain rate. A similar decrease of the plane strain fracture toughness with increasing strain rate is expected. Adiabatic heating and consequent repression of the martensite formation is suggested as the principal responsible mechanism.

TABLE OF CONTENTS

LIST OF FIGURES

LIST OF TABLES

Tables

I. INTRODUCTION

High stress transformation plasticity offers a means of increasing the strength as well as the ductility and toughness of steels (1,2). The additional energy absorption associated with the martensitic transformation during deformation is responsible for the enhanced fracture toughness (3). Prior studies at Syracuse University (4,5) have shown that the martensite content at fracture is a function of the test temperature and that the notch toughness is strongly temperature dependent. Gold and Koppenaal(6) have reported that TRIP steel exhibited embrittlement at a specific strain rate and testing temperature. The studies by Azrin et al.(7), Weiss et al.(4) and Zackay et al. (1) have shown that an optimum combination of strength, toughness and fatigue crack growth resistance required careful control of austenite metastability with respect to the service condition. For example, a TRIP steel that exhibits high strength and toughness under relatively low strain rates at room temperature may suffer a significant loss of uniform ductility at very high strain rates. Also the same TRIP steel may be inferior in fatigue crack propagation resistance to an ultra high strength material.

The studies conducted to date indicate that TRIP steels may be "tailor-made" to possess a unique combination of properties that may make them ideally suited for special critical applications. Since their mechanical properties strongly depend on the inter-relation between deformation and the martensitic transformation, a detailed understanding of these phenomena is required.

The fracture toughness as a function of stress state (plane stress - plane strain) and strain rate is of particular interest. To determine these properties with the recommended procedures, e.g. ASTM E 399, is usually time consuming and expensive. The difficulty in producing TRIP steels of sufficient thickness and the well known difficulties in machining TRIP steels lend further impetus to explore other avenues of assessing the fracture toughness of TRIP steels.

It was therefore decided to obtain information about the fracture toughness as a function of strain rate indirectly from bulge tests at various strain rates, including strain rates corresponding to explosive loading. The feasibility of this approach has been demonstrated through a series of research programs at Syracuse University(8,9). Accordingly the fracture toughness is related to the true effective fracture strain as measured in an equibiaxial bulge test, $\alpha = \sigma_2/\sigma_1 = 1$, $\beta = \sigma_3/\sigma_1 = 0$, $\varepsilon_{F, \alpha = 1, \beta = 0}$, through

$$K_{IC} = 147 \ \overline{\varepsilon}_{F, \alpha = 1, \beta = 0} \quad KSI\sqrt{in}$$

$$= 162 \ \overline{\varepsilon}_{F, \alpha = 1, \beta = 0} \quad MN \ m^{-3/2}$$

While there exists some scatter in the data that led to the above relation-
ship characterized by a relative standard deviation of 33 percent[8], the
expected scatter with respect to the relative influence of strain rate from
one heat and process lot of the TRIP steel studied is expected to be much
smaller, so that an e.g. 10 percent variation in bulge ductility for a change
in strain rate by e.g. 3 orders of magnitude will closely reflect an identi-
cal change in fracture toughness[8,9]. It should be further pointed out that
a method for estimating fracture toughness values for other than plane strain
conditions (i.e. specimen thickness effects and "R Curves") from bulge duc-
tility values[10] has also been proposed and appears to be in agreement with
R Curves determined from standard techniques (9).

Early in the testing program of the TRIP steel the very strong direc-
tional dependence of the fracture ductility was observed as illustrated by
the results of the tensile tests in the longitudinal and the transverse direc-
tion on 79% warm-work TRIP steel. While the true tensile fracture strain in
the longitudinal direction is 0.70, the transverse fracture strain is only
0.34. It was therefore necessary to develop a biaxial test that allows the
selection of a testing direction, which can also be performed at a wide range
of strain rates. The stress state requirement for such a test is $\sigma_1 > \sigma_2$
and $\sigma_2/\sigma_1 \geq 0.5$ to insure that fracture occurs in the longitudinal direction.

Two configurations readily meet this objective, a bulge test through an el-
liptical opening and a plane strain tensile test (11). Both types of tests
were developed and conducted as part of the program and are described in
Section III, Test Procedures.

II. MATERIALS

Prior to the availability of a specially prepared TRIP steel by AMMRC
(Army Materials and Mechanics Research Center), tests were conducted on plates
of TRIP steel available from an earlier program. The chemical compositions
of all materials tested, TRIP steel plate, sheets of TRIP steel and 300M
steel, are listed in Table 1. From the prior program the TRIP steel plate (4)
was induction-melted under a blanket of Argon. The 203 mm X 203 mm X 432 mm
(8" X 8" X 17") cast ingot was heated to 1177°C (2150°F); soaked for 2 hours
and hammer forged to 70 mm (2-3/4") thick X 152 mm (6") wide. The 70 mm
(2-3/4") thick plate material was hot rolled at 1177°C (2150°F) to 38 mm (1-1/2")
thick. The material was austenitized at 1205°C (2200°F) for 1 hour and ice
brine quenched. The plate was warm worked 80% at 425°C (800°F), then it was
cold worked 5%. The finished plate was tempered at 350°C (660°F) for 1 hour.

The major portion of this study was conducted on TRIP steel and 300M
steel supplied by AMMRC. Approximately 25 Kg (58 lbs.) 300M steel, 203 mm X
305 mm X 50 mm (8" X 12" X 2"); and approximately 62.5 Kg (138 lbs.) TRIP steel
in the as-cast condition, 203 mm X 203 mm X 216 mm (8" X 8" X 8-1/2"), were re-
ceived. The 300M steel and the TRIP steel were made by the Electro-Slag Re-
melting (ESR) method at AMMRC.

2

The 300M steel was hot rolled by the Allegheny Ludlum Steel Corporation to 3.2 mm (0.125") thick and approximately 381 mm (15") wide. The 300M steel was heat-treated to two conditions:

(1) Austenitizing at 900°C for 30 minutes followed by continuous cooling to room temperature in air at a cooling rate equal to that achieved at the midpoint of a one-inch thick plate during cooling in still air. To achieve this the 3 mm (0.125") 300M steel was sandwiched between two 13 mm thick hot rolled steel plates, as illustrated in Figure 1. The entire heat treatment was performed on this sandwich.

(2) Austenitizing at 900°C for 30 minutes, followed by isothermal transformation at 350°C for 20 minutes, and water quench. The isothermal transformation time was chosen to produce the maximum retained austenite as determined by X-ray analysis.

The TRIP steel ingot was processed by Allegheny Ludlum Steel Corporation. The detail processing history is described in Appendix I. After the final process four different warm-work conditions at two different thicknesses were available for the program, as listed below.

Material Designation	Reduction of Thickness	Final Thickness mm (inches)
A 0	no reduction	2.03 (0.080)
A 1	79%	1.55 (0.061)
A 2	30%	1.55 (0.061)
A 3	11%	1.55 (0.061)
B 0	no reduction	3.96 (0.156)
B 1	80%	3.17 (0.125)
B 2	38%	3.17 (0.125)
B 3	12%	3.15 (0.124)

The retained austenite content of the 300M steel under two different heat-treated conditions was obtained by X-ray diffraction(12) using CoK_α radiation. The values of the retained austenite of the isothermally transformed and normalized 300M steel were 15.1% and 6.5% respectively. The procedure was calibrated against the 4% austenite 96% ferrite standard supplied by the National Bureau of Standards.

III. TEST PROCEDURES

Ten types of tests were conducted on the 300M steel and TRIP steel to characterize the materials and to study the effect of strain rate on the ductility under multi-axial stress states. They are:

(1) Hardness tests

(2) Uniaxial tensile tests ($\alpha = \sigma_2/\sigma_1 = 0$ and ∞)

(3) Uniaxial tapered tensile tests ($\alpha = 0$)

(4) Hydraulic biaxial bulge tests ($\alpha = 1, \dot{\varepsilon} = 10^{-4}$ sec^{-1})

(5) Hydraulic biaxial bulge tests at medium strain rate
($\alpha = 1, \dot{\varepsilon} = 10^{-1}$ sec^{-1})

(6) Explosive hydraulic biaxial bulge tests ($\alpha = 1, \dot{\varepsilon} = 10^3$ sec^{-1})

(7) Explosive elliptical bulge tests ($\alpha = 0.9, \dot{\varepsilon} = 10^3$ sec^{-1})

(8) Plane strain tensile tests ($\alpha = 1/2, \dot{\varepsilon} = 10^{-4}$ sec^{-1})

(9) Plane strain tensile tests at medium strain ($\alpha = 1/2, \dot{\varepsilon} = 10^{-1}$ sec^{-1})

(10) Explosive plane strain tensile tests ($\alpha = 1/2, \dot{\varepsilon} = 10^3$ sec^{-1})

The stress ratios, α, of 0, 1/2 and 0.9 correspond to the tests in the longitudinal direction; $\alpha = 1$ represents an equibiaxial bulge test and $\alpha = \infty$ corresponds to a test in the transverse direction. Only the A-series of TRIP steel specimens was used in this test program.

Table II represents the test matrix and lists the number of specimens conducted for each test type - material combination.

For the TRIP steel plate, hardness tests with ball indentors and various loads were performed to obtain some information on the flow curve of the material. The specimen is a 25 X 12 X 7 mm block cut from the TRIP steel plate. The hardness tests were performed on three faces of the specimen, on the surface perpendicular to the rolling direction, on the plate surface and on the plate side face. The surfaces were mechanically polished. The specimen was tested on a Greiss hardness testing machine with loads of 20, 40, 50, 120, 140 and 187.5 Kg. The relationship between the applied load and the diameter of the indentation followed Meyer's law which is:

$$P = Kd^n$$

where P = applied load, kg
       d = diameter of indentation, mm
The plots of log P vs. log d are shown in Figure 2.
The amount of true strain, ε, is obtained from (13).

$$\varepsilon = 0.3\left(\frac{d}{D}\right)$$

4

where $D = 1.59$ mm ($1/16"$), the diameter of the ball indentor. The flow stress Y is calculated from

$$Y = \frac{H}{2.7} \ (Kg/mm^2)$$

where $H = 4P/\pi d^2$, Meyer hardness.
For the SI units, the flow stress Y is:

$$Y = 3.63 \ H \ (MPa)$$

Using these relations one can obtain some points on the stress strain curve in the plastic range.

Uniaxial Tensile Tests

Uniaxial tensile tests were conducted on sheet specimens shown in Figure 3. The effective fracture strain, $\bar{\epsilon}_F$, was calculated using:

$$\bar{\epsilon}_F = \epsilon_{1_F} = \ln \frac{A_o}{A_f}$$

where A_o is the initial cross sectional area and A_f is the final cross sectional area.

Uniaxial Tapered Tensile Tests

Uniaxial tapered tensile tests were performed on sheet specimens illustrated in Figure 4. Indentations were made every 5 mm (0.2") along the axis of the tapered section to serve as reference marks. A line was drawn perpendicular to the axis and through each indentation. A point micrometer was used to measure the width and the thickness at each line. The true strain at each line was calculated using:

$$\bar{\epsilon}_F = \epsilon_1 = \ln \frac{A_o}{A_f}$$

The maximum true stress at each line was calculated using:

$$\sigma = \frac{P}{A_f}$$

where P is the maximum load recorded during the test. This type of specimen is well suited to obtain the true stress vs. true plastic strain curve up to the tensile instability strain, ϵ_n.

5

Hydraulic Biaxial Bulge Test

The hydrualic bulge test fixture is schematically illustrated in Figure 5. The system consists of a cylinder, a piston, a top support and a set of flanges. The cylinder is pressurized by placing the entire system in a Baldwin Testing Machine. The top flange is held immobile by a fixed crosshead and a compressive load is applied to the piston until the specimen fractures. In order to prevent hydraulic oil leakage during testing an O-ring is used between the specimen and the cylinder and between the piston and the cylinder wall.

The hydraulic bulge specimen configuration is shown in Figure 6. The specimens were either machine ground so that the variation in thickness was no greater than 2 percent or in the as-received condition (without grinding to remove the surface layer). In the central region of the specimen, where the measurements were made, the thickness typically was uniform to within 0.03 mm. The fracture ductility was determined from:

$$\bar{\epsilon}_F = \epsilon_{3_F} = -\ln\frac{t_f}{t_o}$$

$$\epsilon_{1_F} = \epsilon_{2_F} = -\frac{\epsilon_{3_F}}{2}$$

where t_o is the initial thickness and t_f the final thickness.

The 300M steel hydraulic bulge specimens were heat-treated and machine ground to the final thickness.

Hydraulic Biaxial Bulge Tests at Medium Strain Rates

This hydraulic biaxial bulge test is essentially the same as the one described above except that the piston is driven by the ram of a 900000 Newton hydraulic press with a higher cross head speed, 762 mm./min. (30 in./min.). The test fixture is shown in Figure 7. The specimen configuration is shown in Figure 8, which is a modification of the Azrin-Backofen geometry, developed at Syracuse University (5). A point micrometer was used to measure the thickness.

The fracture ductility was calculated from:

$$\bar{\epsilon}_F = \epsilon_{3_F} = -\ln\frac{t_f}{t_o}$$

$$\epsilon_{1_F} = \epsilon_{2_F} = -\frac{\epsilon_{3_F}}{2}$$

6

The 300M steel hydraulic bulge specimens were heat-treated and machine ground to the final geometry.

Explosive Biaxial Bulge Tests

Explosive biaxial bulge tests were conducted by the system developed by Biegel (14). It is essentially a hydraulic bulge test activated by the pressure generated by igniting a cartridge containing a high-burning rate smokeless powder with an estimated 3500 MPa maximum. The testing fixture is shown in Figure 9. The fracture ductility was calculated from:

$$\bar{\epsilon}_F = \epsilon_{3_F} = -\ln \frac{t_f}{t_o}$$

$$\epsilon_{1_F} = \epsilon_{2_F} = -\frac{\epsilon_{3_F}}{2}$$

The specimen configuration is the same as that of Figure 8. The 300M steel explosive bulge specimens were heat-treated and machine ground to the final geometry.

Directional Biaxial Tests

Because of the inherent directionality of TRIP steel it became necessary to develop biaxial tests for various strain rates, where the principal stresses are not balanced, ($\sigma_1 \neq \sigma_2$). Two possibilities were explored, namely, a hydraulic bulge test through an elliptical opening and a plane strain tensile test. An added condition imposed was that it must be possible to conduct these tests over a wide range of strain rates. Thus, the design and preliminary testing of a suitable fixture for such tests became a major secondary task of the overall program.

A. Elliptical Bulge Test

For this test the stress and strain biaxiality is controlled by the ratio of major and minor axis of the elliptical opening, a/b, and depends on the total strain. Tests on annealed 304 stainless steel specimens, provided with a square grid, were used to experimentally determine the strain biaxiality at the center as a function of geometry. The bulge specimen, with a square grid, made of this stainless steel was bulged with the circular die at a medium strain rate. The grid at the apex of the bulge extended equally in both directions indicating that this stainless steel is mechanically isotropic. Finally, a geometry of a/b = 3.00

was chosen. This produced a strain biaxiality gradually decreasing with increasing strain to approximately $\varepsilon_2/\varepsilon_1 = 0.75$, Figure 10, or a stress biaxiality of approximately $\sigma_2/\sigma_1 = \alpha = 0.9$ (15) for an isotropic material. The geometry of the elliptical die is shown in Figure 11. Although the stress ratio achieved was still close to unity, the test was sufficiently directional to produce fracture in the direction normal to the larger principal stress. For this geometry the fracture strain is given by:

$$\bar{\varepsilon}_F = \varepsilon_{3_F} = -\ln \frac{t_f}{t_o}$$

These tests can be conducted over a range of strain rates including those using smokeless powder as the activating medium.

B. Plane Strain Tensile Tests

The plane strain tensile test uses a test specimen containing face notches. Such a configuration has been widely used for material characterizations in biaxial tension (11). Part of the task consisted of developing a test set-up for conducting a plane strain tensile test at very high strain rates. A solution to this problem was achieved by designing a test specimen that could be pulled hydraulically in a pressure chamber. The specimen geometry and the test chamber are illustrated in Figures 12 and 13 respectively. The specimen was held by two rapidly movable grips inside the test chamber. Gun powder was used to generate the high pressure required to produce a high strain rate. This pressure applied force and motion to the movable cylindrical grips resulting in the fracture of the specimen. The plane strain tensile test at medium strain rate is essentially the same as the plane strain tensile test at high strain rate, only the hydraulic pressure is generated by a moving piston instead of gunpowder. The piston is driven by the ram of a 900000 Newton (100 ton) hydraulic press with a crosshead speed of 762 mm/min. The test fixture is shown in Figure 14. The plane strain tensile tests at a low strain rate were conducted in an Instron testing machine. The crosshead speed is 0.51 mm/min. The fracture strain is given by:

$$\bar{\varepsilon}_F = \frac{2}{\sqrt{3}} \varepsilon_{1F}; \; \varepsilon_2 = 0$$

$$\varepsilon_{1_F} = -\varepsilon_{3_F} = -\ln \frac{t_f}{t_o}$$

The initial thickness of the specimen was measured by using a point micrometer. The final thickness of the specimen was measured under a traveling microscope with a magnification of 35X. The scale of the traveling microscope was calibrated against a standard supplied by the optical company before taking the measurements. The accuracy of the final thickness measurement is within 5 μm.

IV. RESULTS AND DISCUSSION

Results

Hardness Tests

Hardness tests with a 1.59 mm (1/16 in.) indentor and loads varying from 20 to 187.5 Kg were performed to determine parts of the flow curve following the procedure attempted in a prior research program under AMMRC sponsorship[16]. The results are compared with the true stress-true strain curve obtained in the previous TRIP program[4] and are presented in Figure 15. The values of flow stress obtained on the two faces parallel to the rolling direction were higher than those obtained on the face perpendicular to the rolling direction. The observed discrepancy suggests that the proposed correlation[16] does not apply well to TRIP steels.

Tensile Tests

300M Steel

Uniaxial tensile tests and uniaxial tapered tensile tests were performed to obtain the true stress-true strain curves of the TRIP steel (four warm-work conditions) and the 300M steel (two heat-treat conditions). The results are given in Tables III, IV and V. The true stress-true strain curves for the 300M steel are shown in Figure 16. Young's moduli of the two heat-treat conditions for the 300M steel are $E = 1.76 \times 10^5$ MPa for the isothermally transformed 300M steel and $E = 1.50 \times 10^5$ MPa for the normalized 300M steel. The fracture stress and strain of the normalized 300M steel is about 25% above that of the isothermally transformed 300M steel. Before the test the amount of retained austenite of isothermally transformed and normalized 300M steels is 15.1% and 6.5% respectively. After fracturing the amount of retained austenite near the fracture surface of all 300M steel specimens is not measurable by X-ray, i.e., close to zero.

TRIP Steel

The true stress-true strain curves of the TRIP steel (four conditions) in the longitudinal direction are shown in Figure 17. The tensile properties of TRIP steel (four conditions) are presented in Table IV. The true stress-true

strain curves of the TRIP steels were obtained by pulling tapered tensile specimens in the Instron Testing Machine. The crosshead speed was 0.51 mm (0.02 in.)/min. for all tests. Lüders bands were formed in the straight section of the tapered tensile specimens during the early stages of the tests and propagated into the tapered section. The Lüders bands propagated through the entire tapered section of the 0% warm-work TRIP steel tapered tensile specimen, through about 1/3 of the tapered section in the 79% warm-work tapered tensile specimen, and through 1/2 of the tapered section in the 30% warm-work tapered tensile specimen. The true stress-true strain curve for 11% warm-work tapered tensile specimen could only be determined for strains above 0.15. Another tensile test was conducted to obtain the entire true stress-true strain curve. The tapered tensile specimens of 79%, 30% and 11% warm-work TRIP steel materials fractured within the straight section, but the tapered tensile specimen of 0% warm-work TRIP steel fractured at the bottom of the gage length, at the fillet, at a strain which was less than the maximum strain obtained from the same specimen; therefore, the true fracture strain for the 0% warm-work TRIP steel could not be determined from this test.

A tensile test was conducted on the 79% warm-work TRIP steel in the transverse direction. The true stress-true strain curves of the 79% warm-work TRIP steel in longitudinal and transverse directions are compared in Figure 18, and their tensile properties are listed in Table V. The fracture strain in the longitudinal direction is twice the fracture strain in the transverse direction. The fracture stress in the longitudinal direction is about 1.5 times that in the transverse direction. This strong directionality made it necessary to develop biaxial test methods for several strain rates where the principal stresses are not balanced ($\sigma_2/\sigma_1 \neq 1$).

The data indicate that the fractures stress of the TRIP steel increases as a function of the amount of warm-work. The fracture ductility of the TRIP steel increases to its maximum value at 30% reduction of thickness and then decreases, Figure 19.

Bulge Tests

300M Steel

The results of the hydraulic biaxial bulge test at three strain rates are given in Table VI and VII. The quoted strain rate represents an approximate value which is obtained by dividing the fracture strain by the test time. Two hydraulic bulge tests at low strain rates ($\dot{\epsilon} \approx 10^{-4}$ sec^{-1}) were conducted on the isothermally transformed 300M Steel - both fractured at the apex of the bulge; one broke into three pieces and the other broke into four pieces. The fracture zone of one specimen extended into the hold-down area. Otherwise the two tests gave the same results with a fracture strain of 0.11 and a uniform strain of 0.09 (as measured some distance away from the fracture point).

One hydraulic bulge test at low strain rate ($\dot{\epsilon} \approx 10^{-4}$ sec^{-1}) was conducted on the normalized 300M steel. The specimen fractured at the apex of the

10

bulge and extended through the entire specimen resulting in two segments. One segment of the bulged region was separated from the main portion of that segment. The fracture strain is 0.18 and the uniform strain is 0.13.

One hydraulic bulge test at medium strain rate ($\dot{\varepsilon} \approx 10^{-1}$ sec^{-1}) was conducted on each heat-treat condition of 300M steel. The fracture line of the isothermally transformed 300M steel specimen formed an "S" shape, with a fracture strain of 0.14. The normalized 300M steel specimen broke into three pieces with the fracture strain of 0.21. Both 300M steel specimens fractured at the apex of the bulge.

Three explosive bulge tests were performed on the isothermally transformed 300M steel. All three specimens fractured on the apex of the bulge, two broke into four pieces and the other broke into five pieces. The fracture strains obtained from the three tests are 0.28, 0.29 and 0.28. The average value was 0.28.

One explosive bulge test was conducted on the normalized 300M steel. The thickness of the specimen was not uniform and the specimen did not fracture at the apex of the bulge. The fracture strain (0.17) obtained from this specimen did not appear to be representative of the material.

TRIP Steel:

Hydraulic bulge tests at low strain rate ($\dot{\varepsilon} \approx 10^{-4}$ sec^{-1}) were also conducted on the TRIP steel sheet (four warm-work conditions) in the as-received condition (without grinding to remove the surface layer). The thickness of these four specimens was within 0.05 mm. The 0%, 30% and 79% warm-work TRIP steel specimens fractured at the apex of the bulge with the fracture strains of 0.58, 0.40 and 0.32 respectively. Two 11% warm-work TRIP steel specimens were tested. One of them did not fracture at the apex of the bulge but on the side, half-way towards the bulge where the stress state is $\alpha \neq 1$ and $\beta \neq 0$. The fracture strain (0.40) obtained from this specimen cannot be regarded as the true value of bulge ductility. The other one fractured at the apex of the bulge with fracture strain of 0.45.

Prior to the availability of the new material explosive bulge tests were performed on the TRIP steel plate. The first specimen was machined and ground to a final thickness of 1.14 mm. The specimen was strained twice without fracture. The thickness at the apex of the bulge was 1.04 mm. This is a strain of 0.09. The bulge extended 5.46 mm above the base plane of the specimen.

The second specimen was machined and ground to a 0.64 mm thickness. The thickness at the fracture zone was 0.56 mm for a fracture strain of 0.13. This specimen was also strained twice. The fracture zone extended into the area under the hold down. Two segments of the bulge area were broken away from the rest of the specimen.

11

The third specimen was machined, ground and polished (the direction of the final polish with respect to the rolling direction is uncertain although observation indicates that they were nearly perpendicular). This specimen was also strained twice with a reduction in thickness from 0.65 mm to 0.58 mm in the fracture zone. This is a strain of 0.10. The fracture line did not pass through the apex of the bulge where the final thickness was 0.56 mm with a strain of 0.15. The fracture originated from a hole in the periphery of the specimen (used for hold down during machining). Another fracture started to propagate from another hole at the periphery approximately 90° from the other fracture line. One segment of the bulge was broken away from the main portion of the specimen.

The fourth specimen fractured into two pieces, the fracture zone extending approximately through the center of the specimen and under the hold down. The fracture line coincided with the rolling direction. The original thickness was 0.86 mm and the final thickness was 0.56 for a fracture strain of 0.20. This specimen was polished with the final polishing direction being perpendicular to the rolling direction.

The third and fourth specimens display an elongated 'orange peel' effect with the elongation in the rolling direction. This is attributed to the directionality of the material. Observation under a low power microscope confirms this phenomenon.

The results of the explosive elliptical bulge test on the TRIP steel are given in Table VIII. The major axis of the elliptical die was oriented perpendicular to the longitudinal direction. Fracture in each specimen occurred along the major axis of the elliptical die, perpendicular to the longitudinal direction of the specimen, thus representing a longitudinal test direction. The effective true fracture strains achieved were 0.41, 0.21, 0.33 and 0.36 for 0%, 79%, 30% and 11% warm-work TRIP steel specimens respectively.

Plane Strain Tensile Test

The results of the plane strain tensile test on the TRIP steel, at 3 strain rates, static ($\dot{\varepsilon} = 10^{-4}$ sec^{-1}), medium ($\dot{\varepsilon} = 10^{-1}$ sec^{-1}) and explosive ($\dot{\varepsilon} = 10^3$ sec^{-1}) are presented in Table IX. The low strain rate tests were conducted on the Instron Testing Machine. During this test the crosshead speed was controlled at 0.5 mm./min. for all four tests. The measured plane strain ductilities (the effective true fracture strain for the stress state $\sigma_2/\sigma_1 = 1/2$) were found to be 0.42, 0.50, 0.51 and 0.48 for the 0%, 79%, 30% and 11% warm-work conditions respectively. For the medium strain rate ($\dot{\varepsilon} = 10^{-1}$ sec^{-1}) the results were 0.58, 0.40, 0.45, 0.63 again for the 0%, 79%, 30% and 11% warm-work conditions. The plane strain tensile tests at explosive strain rates were performed using the apparatus illustrated in Figure 13. The effective fracture ductilities measured under these conditions are 0.41, 0.35, 0.38, and 0.47 again for the 0%, 79%, 30% and 11% warm-work conditions respectively.

Discussion

300M Steel

As a result of tensile testing to failure the amount of retained austenite in the 300M steel decreased from 6.5% to 0 for the steel in the normalized condition and from 15.1% to 0 for the steel isothermally transformed to produce a high amount of retained austenite. The results for both heat-treat conditions clearly indicate that practically all the austenite transforms to martensite when specimens are tested to fracture at room temperature. Based on the observation of the transformation of retained austenite it is suggested that the transformation enhanced both the fracture strain and the fracture stress of the 300M steel specimens.

The bulge ductility (effective true fracture strain under equibiaxial bulge test) increases with increasing strain rate from 0.11, as measured under quasi static conditions ($\dot{\varepsilon} \approx 10^{-4}$ sec^{-1}), to 0.29 under explosive conditions ($\dot{\varepsilon} \approx 10^3$ sec^{-1}) for the isothermally transformed steel, Figure 20. A similar result was obtained from Type 301 stainless steel (5). The increase in bulge ductility with increasing strain rate in 300M steel may be attributed to adiabatic heating (17) during the high strain rate test (as no strain localization has been observed).

TRIP Steel

The TRIP steel showed strong evidence of directionality. This required the development of multiaxial tests, for which the principal stresses are not equal, and which are capable of being performed over a range of strain rates. Thus an elliptical explosive bulge test was developed and the plane strain tensile test was adapted to high strain rate (explosive) conditions.

An Aminco-Brenner magne-gage with #3 magnet was used to measure the amount of martensite formed near the fracture face to obtain further information about the relationship between martensite formation, fracture strain and strain rate. Other martensite measurement techniques, such as metallographic and X-ray diffraction, were not used since these are directionally sensitive. Moreover, the metallographic measurement is very time-consuming and highly inaccurate due to the distorted microstructure of the TRIP steel after plastic deformation. Furthermore, since the martensite has a specific orientation to the parent austenite matrix, which is itself highly oriented due to the warm-work, it is not likely that an examination of any one face will yield a representative martensite determination. X-ray diffraction analysis is complicated by the preferred orientation which results from warm-working, and the resulting elongated grain shape makes special diffraction techniques necessary. The magne-gage measurement technique gives an average value of martensite content of the volume under the magnet, and the plastic deformation has little effect on the value measured. Besides, the magne-gage technique is very easy to perform (18).

13

The calibration chart was obtained by using the NBS Thickness Standards (SRM No. 1313 through SRM No. 1320) in accordance with the procedure from the Welding Research Report, July 1, 1972. The accuracy of the measured ferrite content is within 1% when the value obtained is below 10%, above that the accuracy is less [19]. To minimize the edge effect and rough surface effect in the measurement, the broken halves of fracture specimen were put together as close as possible. Due to the limitation of the magnegage the amount of martensite content in a specimen can only be measured up to 20%.

Initially the martensite content of each TRIP steel specimen under the four heat-treat conditions was zero. After the uniaxial tensile tests the amount of martensite content near the fracture face of each tapered tensile specimens of TRIP steel for all four heat-treat conditions was in excess of 20%.

The martensite content near the fracture face in the Clausing specimens of TRIP steel, for the four warm-worked conditions at three strain rates ($\dot{\varepsilon} = 10^{-4}$ sec-1, 10^{-1} sec^{-1} and 10^3 sec^{-1}) are listed in Table X. In general the amount of martensite formed decreases with increasing strain rate, except for the 0% warm worked (solution annealed) condition.

The effective fracture strains obtained from the explosive elliptical bulge tests of the TRIP steel specimen decreases with increasing warm-work (Figure 21). The plane strain ductility of the TRIP steel specimens at high strain rate ($\dot{\varepsilon} = 10^3$ sec^{-1}) and at medium strain rate ($\dot{\varepsilon} = 10^{-1}$ sec^{-1}) first increases and then decreases with increasing warm-work. At low strain rate ($\dot{\varepsilon} = 10^{-4}$ sec^{-1}) the plane strain ductility increases with increasing warm-work (Figure 22). The same kind of variation for increasing warm-work was also observed for the amount of martensite content at the fracture face of the plane strain TRIP steel specimens (Table X). This suggests that both the stability and the M_d temperature of TRIP steel are affected by the amount of warm work during TRIP processing.

The plane strain fracture ductility of TRIP steel decreases with increasing strain rate for the 79% and 30% warm work conditions; this trend is opposite to that found for 300M steel. Again the same trend was also observed for the amount of martensite formed at the fracture face of the plane strain fracture specimens (Table X). For the two lower warm-work conditions, 0% and 11%, the plane strain fracture ductility first increased from the quasistatic to the medium strain rate and then decreased from the medium to the explosive strain rate to a value slightly below that obtained from the quasistatic test (Figure 23).

The decrease of plane strain fracture ductility of high strength TRIP steels, 30% and 79% warm work conditions, with increasing strain rate can probably be attributed to adiabatic heating during the deformation period (7,17), thereby reducing the tendency for martensitic transformation. However, for

14

the two lower warm work conditions, 0% and 11%, the plain strain fracture
ductility and the amount of martensite formed at the fracture face cannot
be explained by adiabatic heating only. Therefore, it is suggested that
these effects are caused by an interplay between adiabatic heating, stability
of metastable austenite in TRIP steel (which increases with increasing tem-
perature) and the effect of warm-work on M_d temperature.

It is expected that the fracture toughness - strain rate behavior will
follow the trend exhibited by the plane strain ductility. This has been
partially confirmed by the result of a ballistic test on a TRIP steel plate [20],
which showed high toughness and ductility under low strain rate conditions, but
very little resistance to penetration under high strain rate conditions.

The stress state also has a strong effect on the effective fracture strain
(Figure 24). The effective true fracture strain of 30% and 79% warm worked
TRIP steel specimens decreased when the stress state changed from $\alpha = 0$ to
$\alpha = 1$ at low strain rate. At high strain rate the effective true fracture
strain of 11%, 30% and 79% warm worked TRIP steel specimen decreased when the
stress state changed from $\alpha = 1/2$ to $\alpha = 0.9$. These results follow the
critical mean stress fracture criterion proposed by Weiss [21]. However, the
results obtained from 0% warm worked TRIP steel specimens at high and low
strain rates do not show the same kind of change with the stress state.

V. SUMMARY

The results of a feasibility test program to characterize the room tem-
perature high strain fracture toughness of ultra high strength 300M steel and
TRIP steel with various amounts of warm-work can be summarized as follows:

1. The basic mechanical properties of the test materials are il-
   lustrated by means of tensile tests on standard and tapered
   tensile specimens. For the 300M steel virtually all retained
   austenite is transformed to martensite at and near the fracture
   site. For the TRIP steel the maximum fracture strength is
   obtained for the 79% warm-work condition. The amounts of mar-
   tensite formed near the tensile fracture face increased from
   zero to more than 20%. (The exact amount can not be obtained
   due to the limitation of the apparatus).

2. The bulge ductility of 300M steel was found to increase with
   increasing strain rate. This was observed for both conditions
   of 300M steel, normalized and isothermally transformed for
   maximum retained austenite. This behavior is similar to that
   observed on Type 301 stainless steel (5). It is believed that
   an increase in bulge ductility at high strain rate can be at-
   tributed to adiabatic heating of the specimens during the
   test. By reference to the previously observed correlation be-
   tween bulge ductility and fracture toughness the present re-

sults indicate that one might expect an increase in fracture toughness with increasing strain rate in 300M steel containing varying amounts of metastable retained austenite.

3. The biaxial ductility of TRIP steel decreases with increasing strain rate for the 79% and 30% warm-work conditions, from approximately 0.50 to approximately 0.37. This trend is opposite to that found for 300M steel. For the two lower warm-work conditions, the plane strain fracture ductility first increases from the static to the medium strain rate and then decreases from the medium to the explosive strain rate to a value slightly below that obtained from the quasi-static test. It is suggested that these effects are caused by an interplay between adiabatic heating, stability of metastable austenite in TRIP steel (which increases with increasing temperature) and the the effect of warm-work on the M_d temperature. It is expected that the fracture toughness - strain rate behavior will follow the trend exhibited by the plane strain ductility.

ACKNOWLEDGEMENT

APPENDIX I

THE THERMOMECHANICAL TREATMENT OF TRIP STEEL
PERFORMED BY
ALLEGHENY LUDLUM STEEL CORPORATION

(1) Sawed to remove 19 mm (3/4") thick slice which was shipped to Syracuse University.

(2) Balance of the material was heated to 1177°C (2150°F) and forged to 102 mm (4") thick X 165 mm (1-1/2") wide X R.L. billet. During forging, rupturing occurred at one end of the billet. The cracks did not propagate to any great depth during subsequent forging to final size.

(3) Billet conditioned completely by grinding. Some fine cracks remained upon one end of the billet after extremely deep conditioning.

(4) Sawed billet into two pieces representing 1/3 and 2/3 volume of material. The piece representing 2/3 the volume contained the residual cracks.

(5) Heated the 2 pieces to 1177°C (2150°F) and hot rolled both pieces to 25 mm (1") thickness. The large piece developed cracks in the area which had contained residual cracks.

(6) Abrasive cut both pieces of material into three equal parts for later processing. Remove the defective material from the larger piece and shipped to Syracuse University. Material at this stage was either hard or very abrasive.

(7) The six pieces, 25 mm (1.0") thickness were conditioned by grinding.

(8) The six pieces were heated to 1177°C (2150°F) hot rolled to the following thicknesses and permanently identified:

	Thickness	
	mm	inches
A 1	8.05	(0.317)
A 2	2.69	(0.106)
A 3	2.03	(0.080)
B 1	16.03	(0.631)
B 2	5.36	(0.211)
B 3	3.96	(0.156)

(9) Each of the pieces in 8 above were either sheared cold or sheared warm into three equal pieces. Two pieces of scrap, 1 piece from each A-3 and B-3 were shipped to Syracuse University in the as hot rolled condition.

(10) The 18 pieces were grit blasted to remove hot work scale.

(11) Pieces were coated with Ceram-guard, solution treated at $1204^{o}C$ ($2200^{o}F$) for 1 hr. in an air atmosphere and water quenched.

(12) Grit blast and light pickle.

(13) All 18 pieces were heated to $480^{o}C$ ($900^{o}F$) and warm-cold rolled to the final thickness.

(14) After the final process four different warm-work conditions at two different thicknesses were available for the program, as listed below.

Material designation	Reduction of thickness	Final thickness mm	inches
A 0	no reduction	2.03	(0.080)
A 1	79%	1.55	(0.061)
A 2	30%	1.55	(0.061)
A 3	11%	1.55	(0.061)
B 0	no reduction	3.96	(0.156)
B 1	80%	3.17	(0.125)
B 2	38%	3.17	(0.125)
B 3	12%	3.15	(0.124)

FIG. 1   SANDWICH ARRANGEMENT FOR 300M STEEL ACHIEVES
THE DESIRED COOLING RATE EQUIVALENT TO THAT AT
MID-THICKNESS OF A 1 INCH THICK PLATE IN STILL AIR
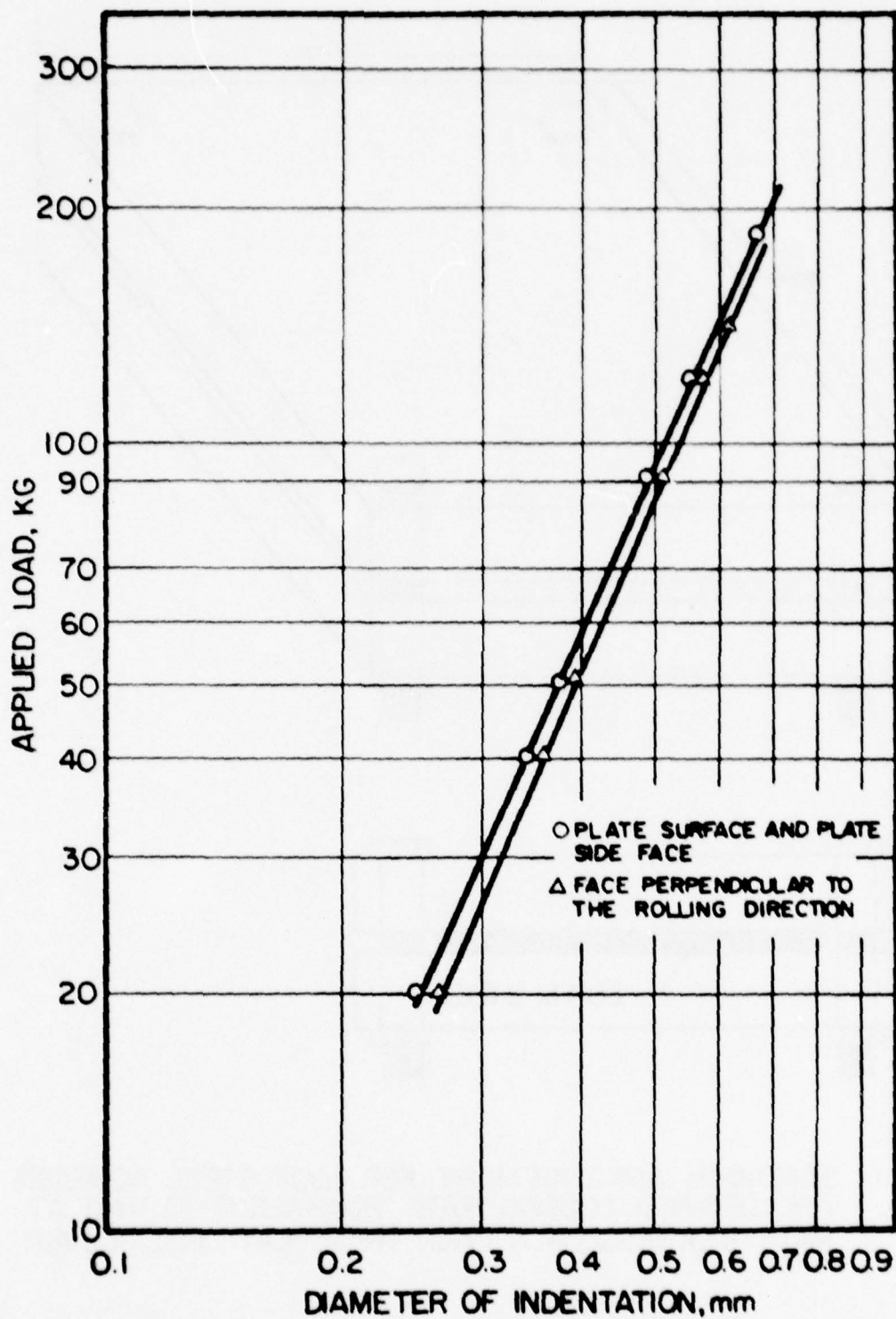
FIG. 2 APPLIED LOAD VS. DIAMETER OF INDENTATION FOR TRIP STEEL PLATE

FIG. 3   TENSILE TEST SPECIMEN

FIG. 4   TAPERED TENSILE SPECIMEN WITH 25mm STRAIGHT SECTION
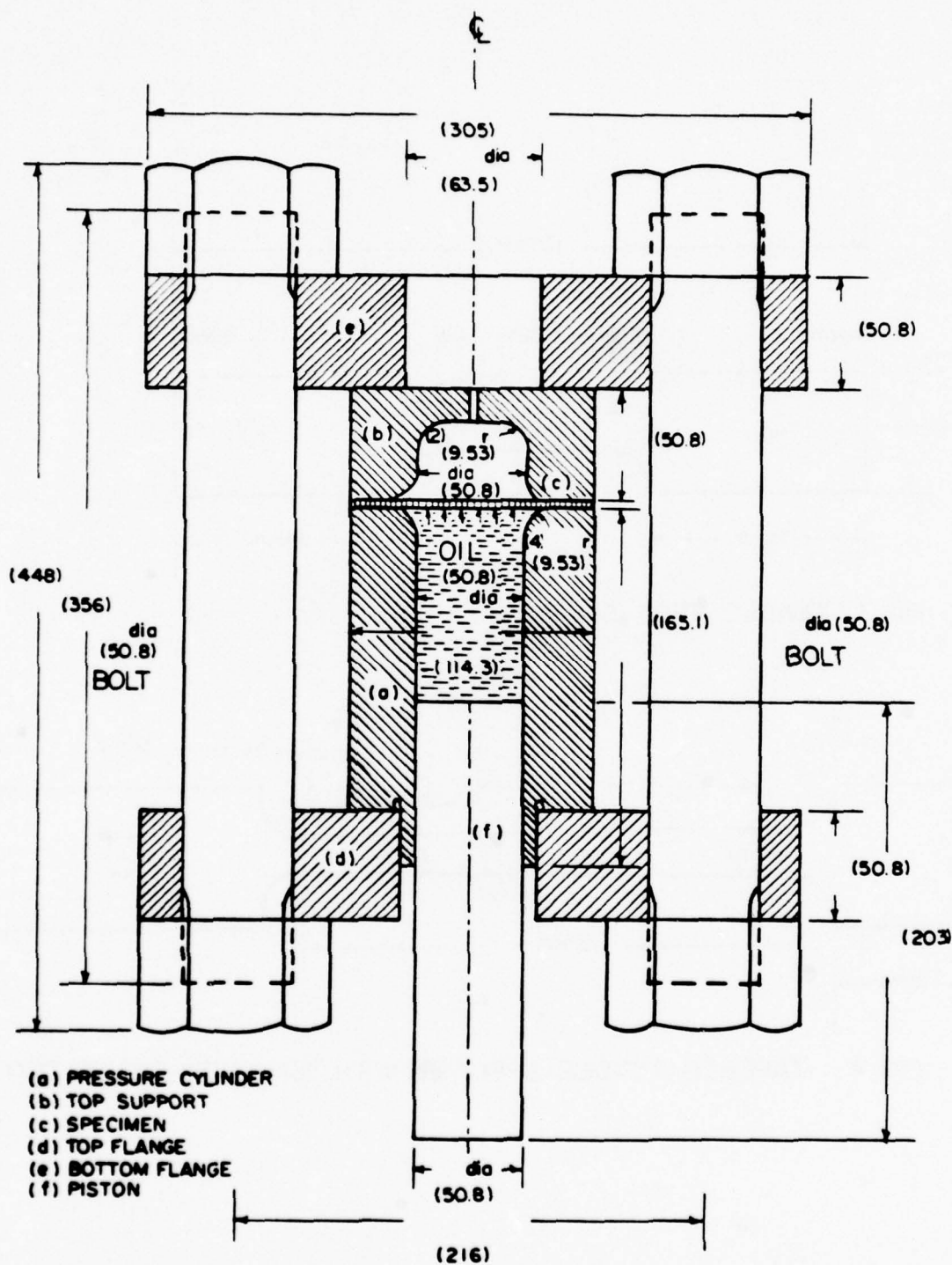
FIG. 5 HYDRAULIC BULGE FIXTURE FOR BALANCED BIAXIAL($\sigma_2/\sigma_1 = 1$, $\sigma_3/\sigma_1 = 0$) TENSION TEST. DIMENSIONS IN ( ) ARE IN mm
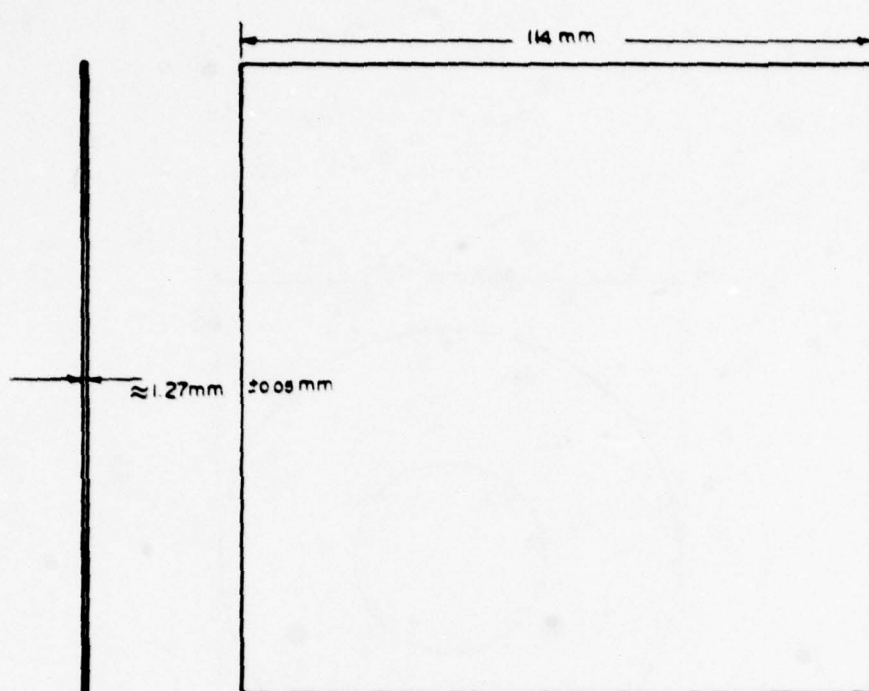
FIG. 6 HYDRAULIC BULGE SPECIMEN
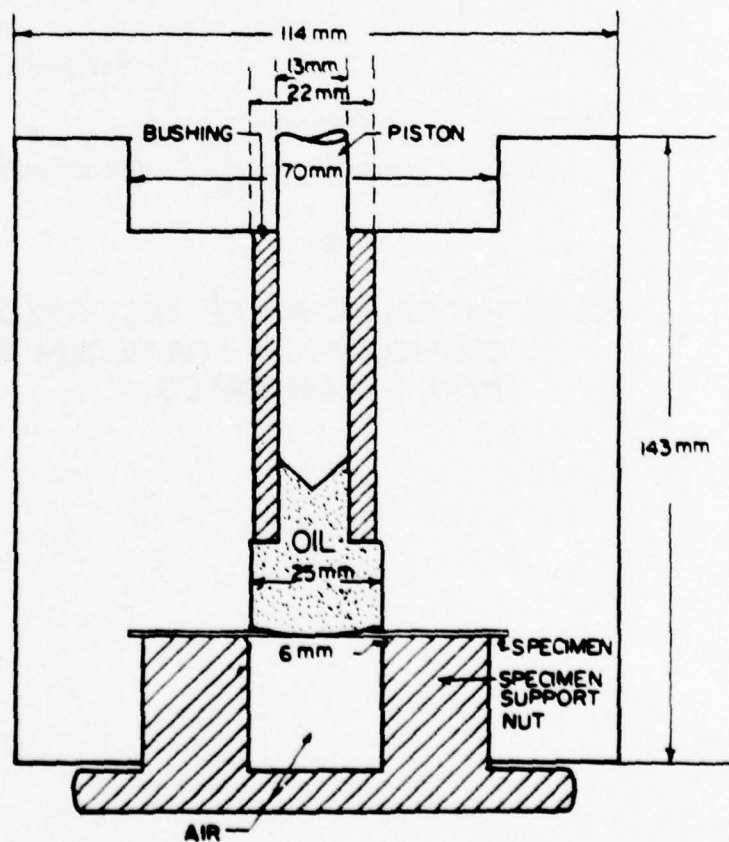
FIG. 7 HYDRAULIC BULGE TEST APPARATUS FOR MEDIUM STRAIN
RATE
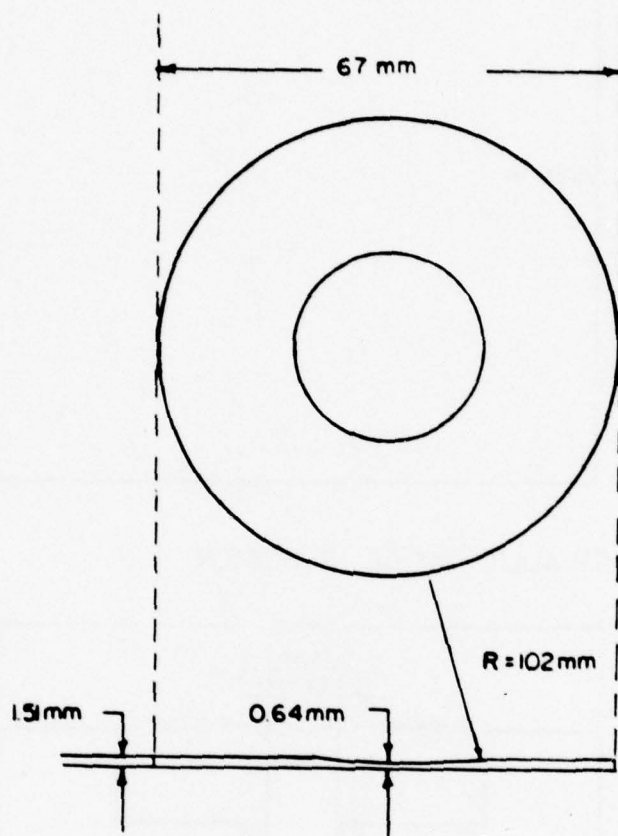
FIG. 8 HYDRAULIC BULGE TEST SPECIMEN
CONFIGURATION FOR MEDIUM AND
HIGH STRAIN RATES
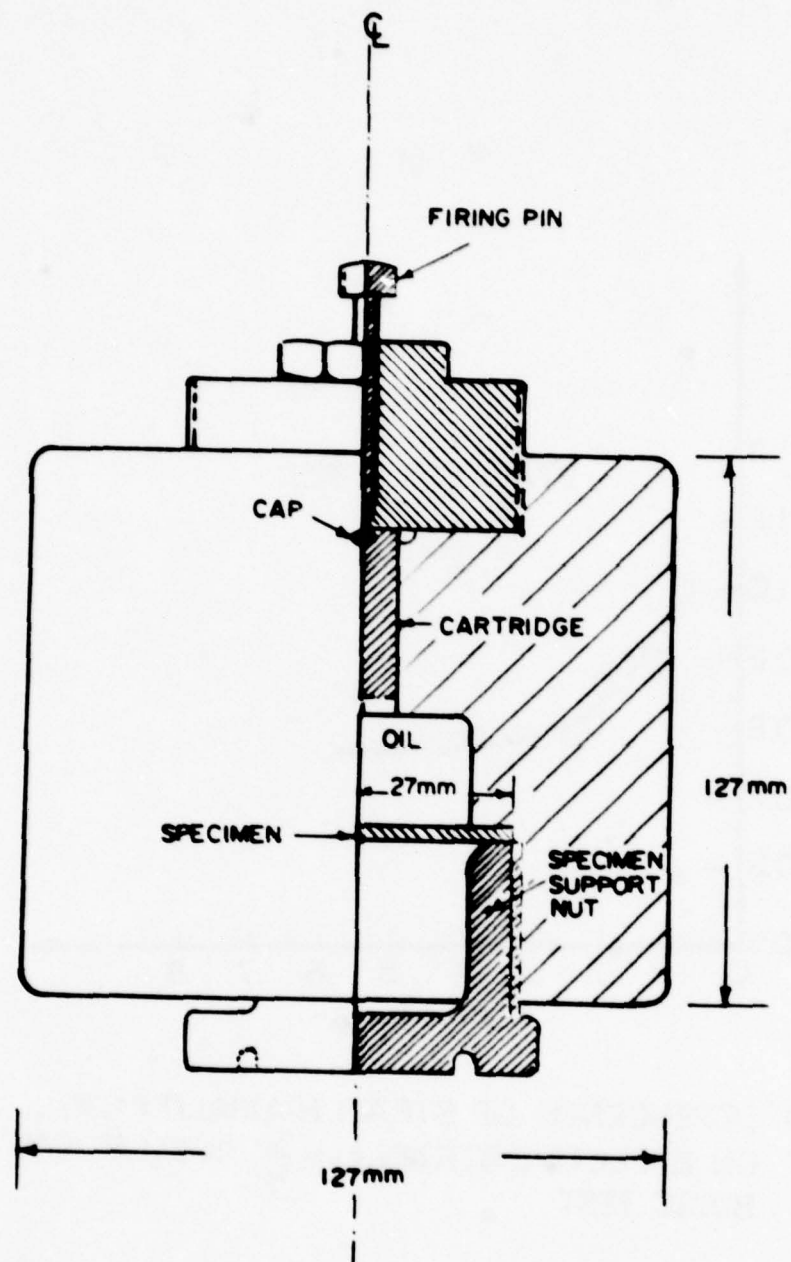
FIG. 9 EXPLOSIVE BULGE TEST APPARATUS
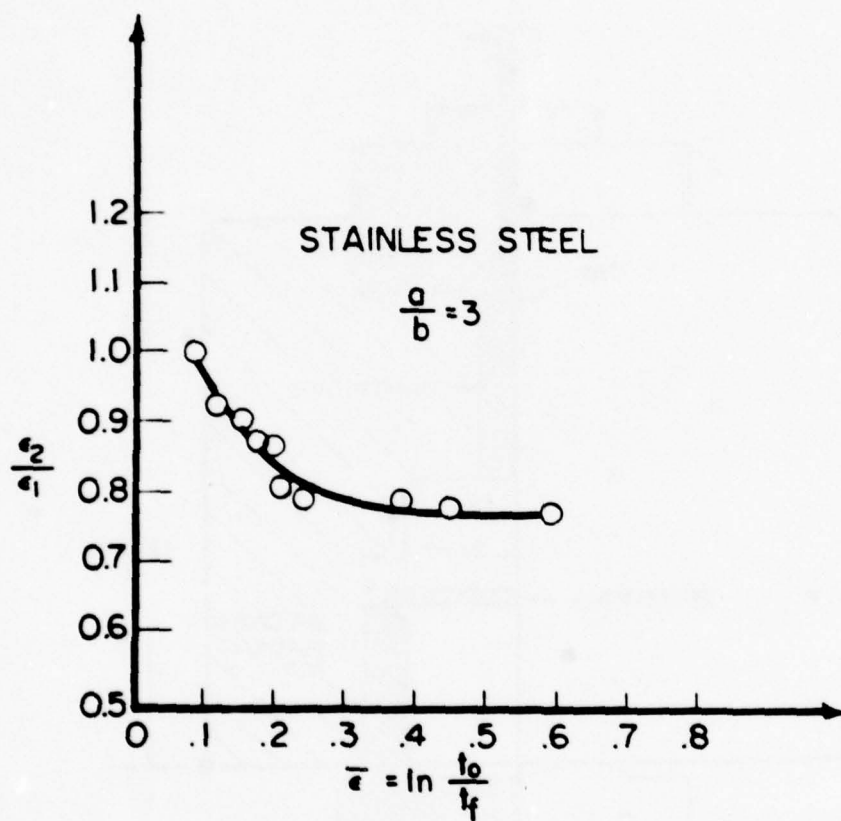
FIG. 10 DEPENDENCE OF STRAIN BIAXIALITY ϵ_2/ϵ_1,
ON EFFECTIVE STRAIN, $\bar{\epsilon} = \ln \frac{t_0}{t_f}$, IN ELLIPTICAL
BULGE TEST
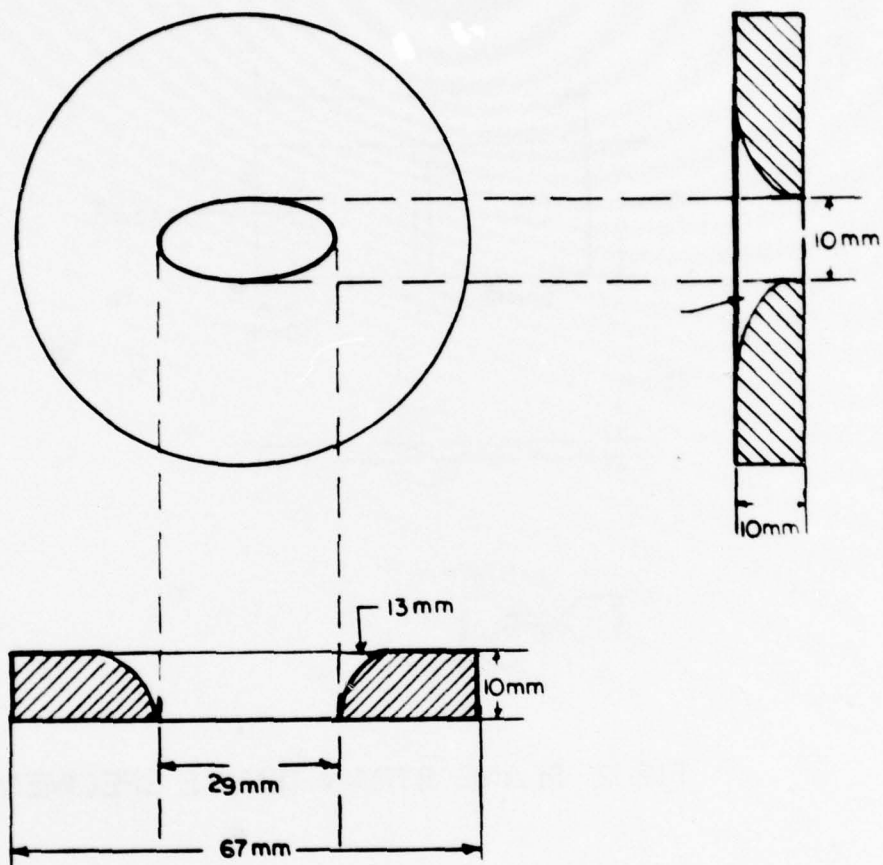
FIG. II GEOMETRY OF THE ELLIPTICAL DIE
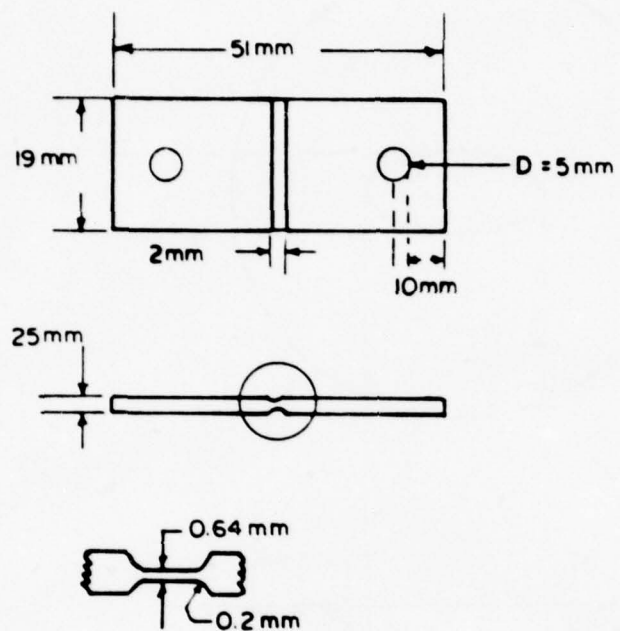
FIG. 12 PLANE STRAIN TENSILE SPECIMEN

TEST BLOCK — CARTRIDGE

25 mm

OIL

PIN ○ | ○ PIN

19 mm
41 mm

GRIP

SPECIMEN

76 mm

SECTION A—A

A

A
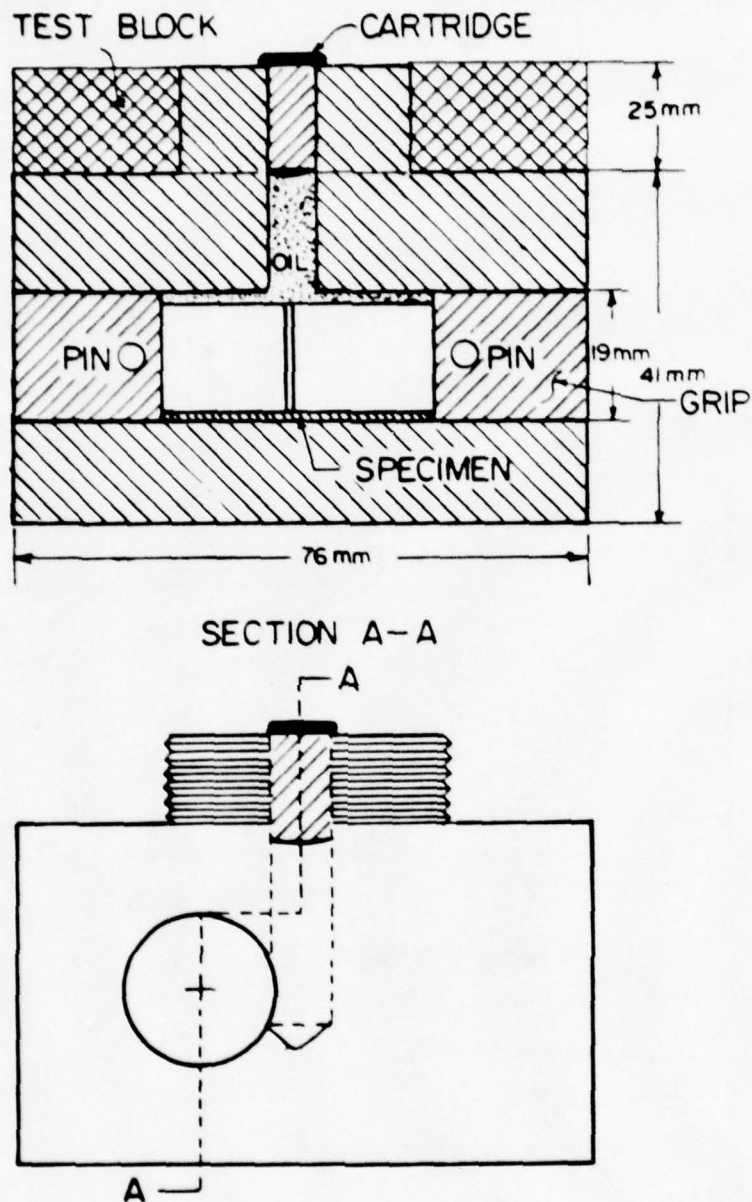
FIG. 13   PLANE STRAIN TENSILE TEST APPARATUS FOR
HIGH STRAIN RATE
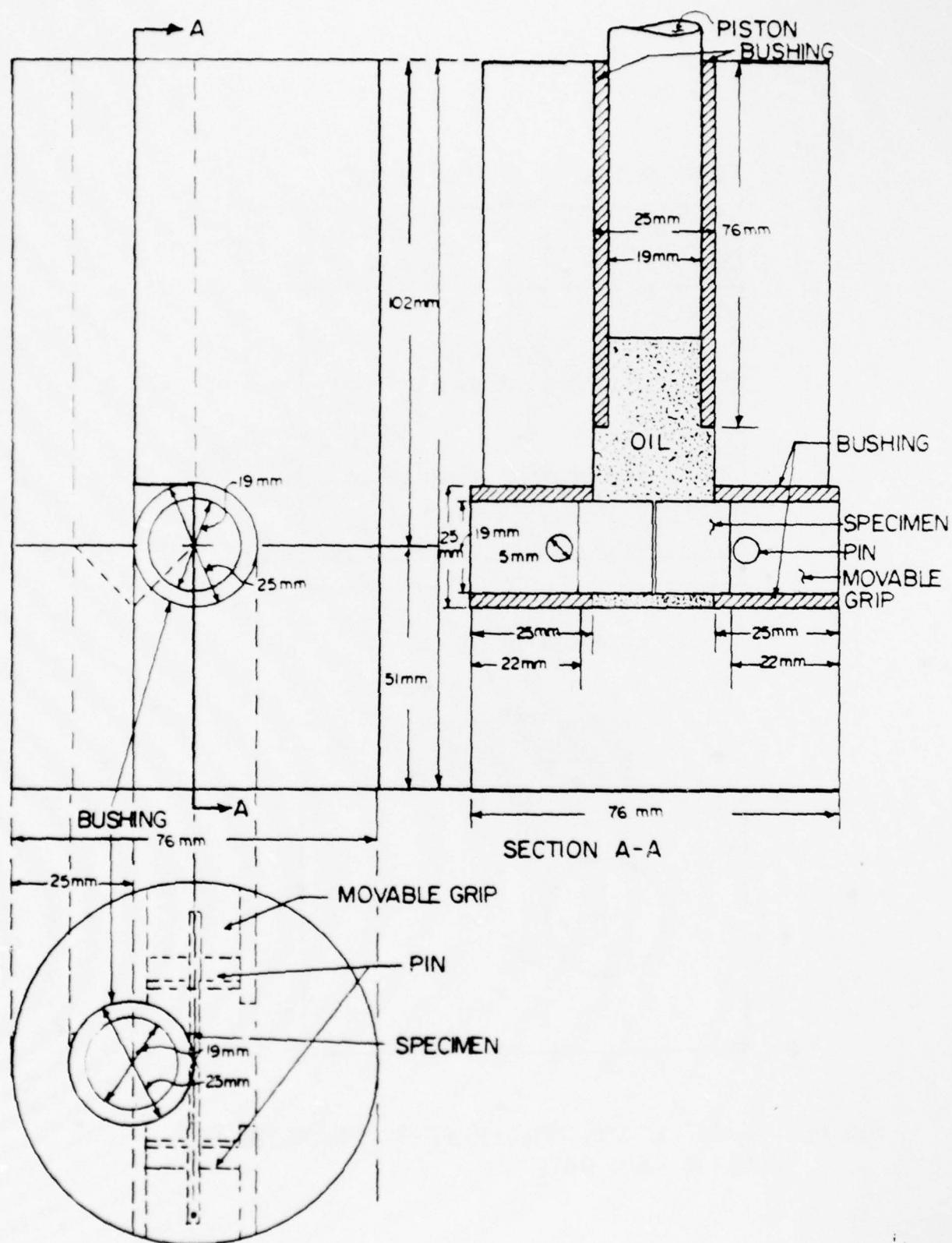
FIG. 14   TESTING APPARATUS FOR THE PLANE STRAIN TENSILE TEST AT
MEDIUM STRAIN RATE

FLOW STRESS Y MPa ⟶

2100

1800

1500

1200

900

600

300

0

TRUE STRESS - TRUE STRAIN
CURVE OBTAINED FROM
PREVIOUS MONOTONIC TENSILE
TEST (REF. 4)

O PLATE SURFACE

☐ FACE PERPENDICULAR TO
THE ROLLING DIRECTION

△ PLATE SIDE FACE

0.05   0.10   0.15   0.20
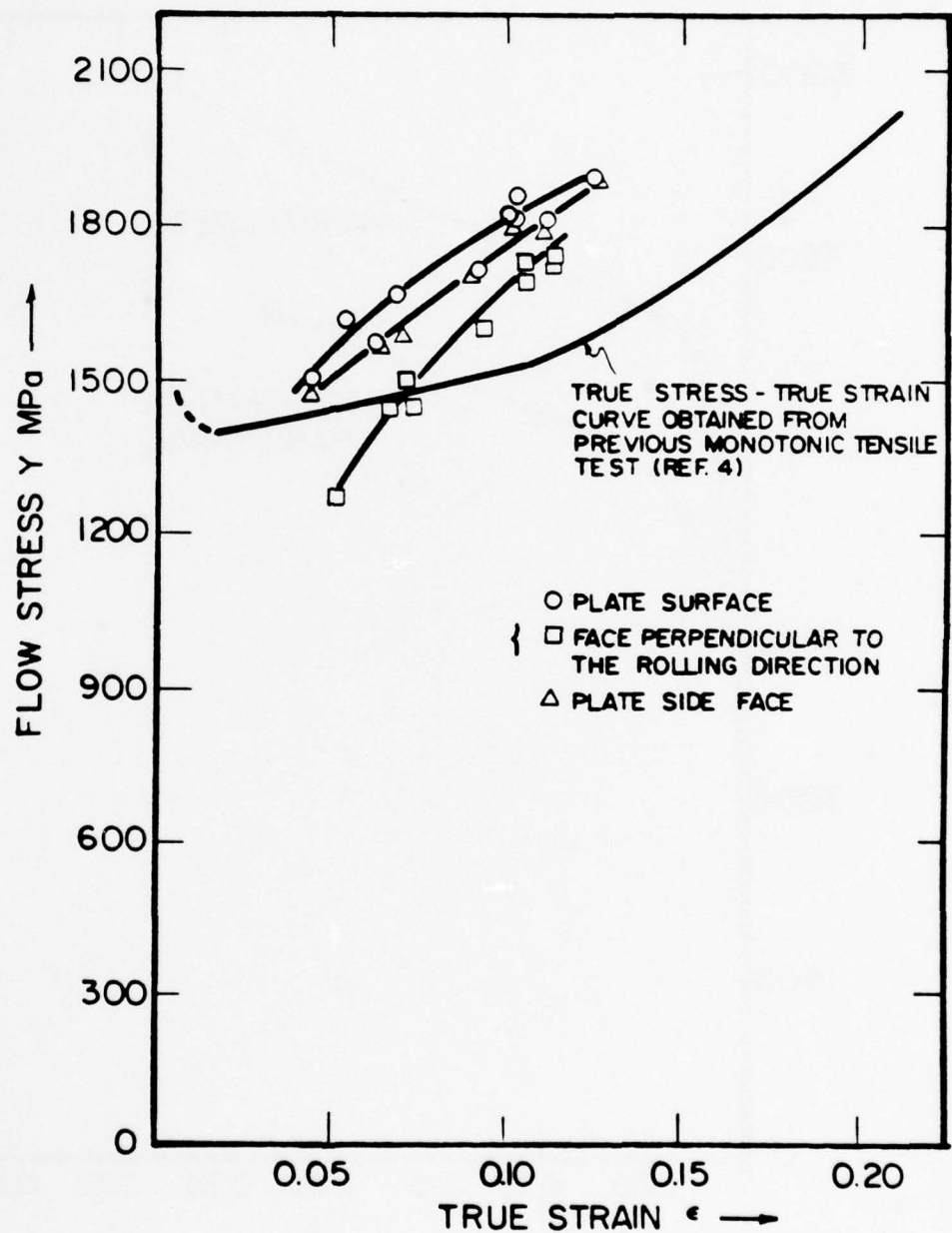
TRUE STRAIN ε ⟶

FIG.15   FLOW STRESS VS. TRUE STRAIN.
COMPARISON OF THE TRUE STRESS-TRUE STRAIN
CURVE OBTAINED FROM PREVIOUS UNIAXIAL
TENSILE TEST (REF. 4) WITH THE STRESS STRAIN DATA
OBTAINED FROM HARDNESS TEST FOR TRIP STEEL
PLATE
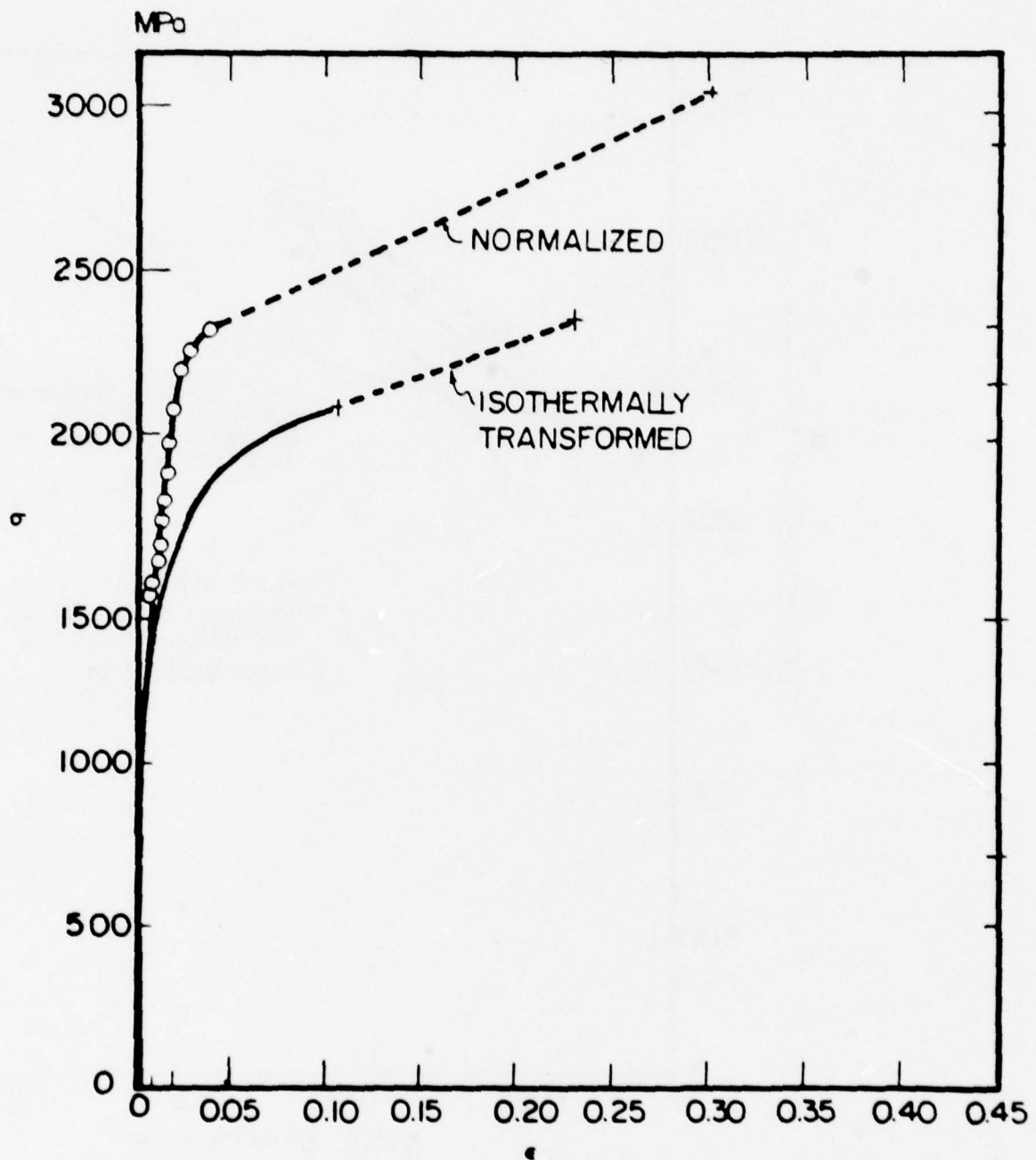
FIG. 16 TRUE STRESS - TRUE STRAIN CURVE OBTAINED FROM THE TAPERED TENSILE SPECIMEN FOR NORMALIZED 300M STEEL AND FROM THE STANDARD TENSILE SPECIMEN FOR ISOTHERMALLY TRANSFORMED 300M STEEL
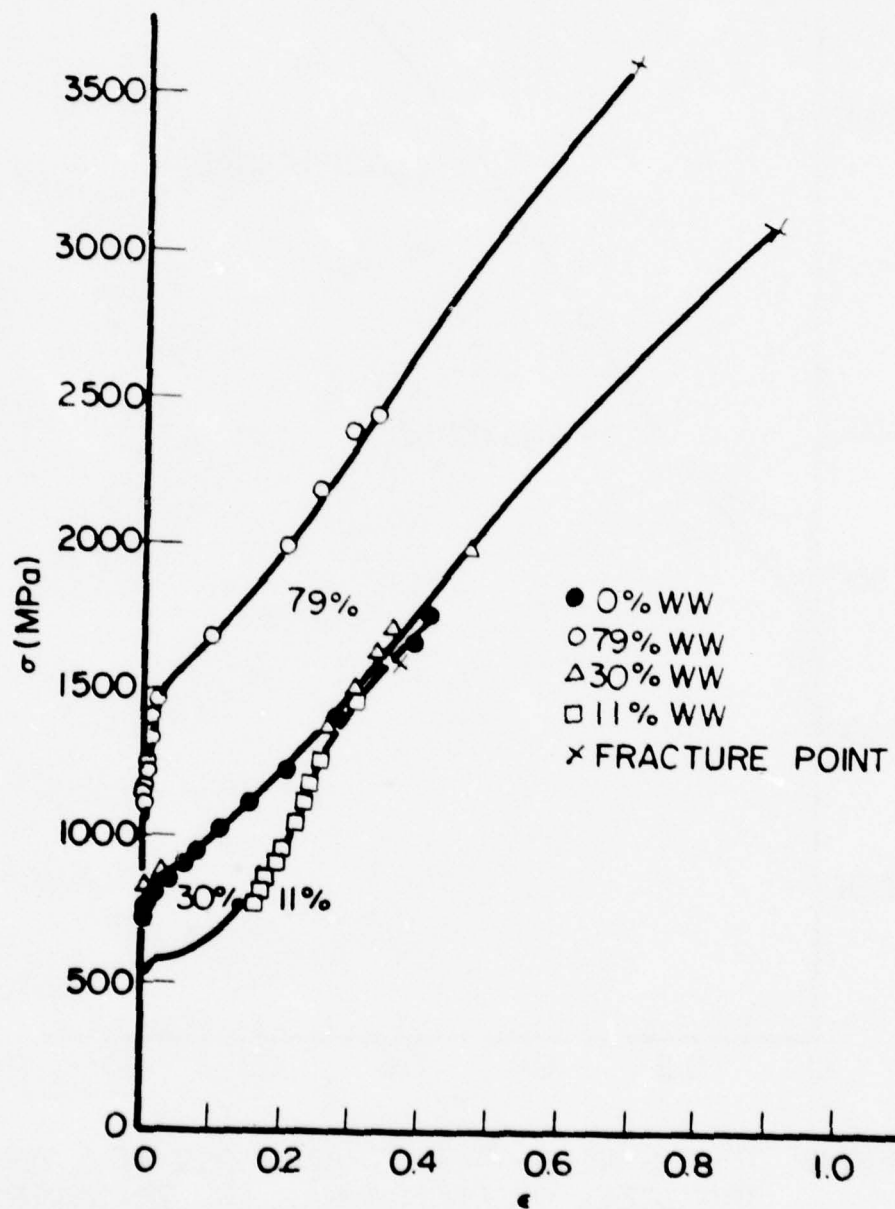
FIG 17 TRUE STRESS VS. TRUE STRAIN CURVES OBTAINED FROM THE TAPERED TENSILE SPECIMENS OF TRIP STEEL
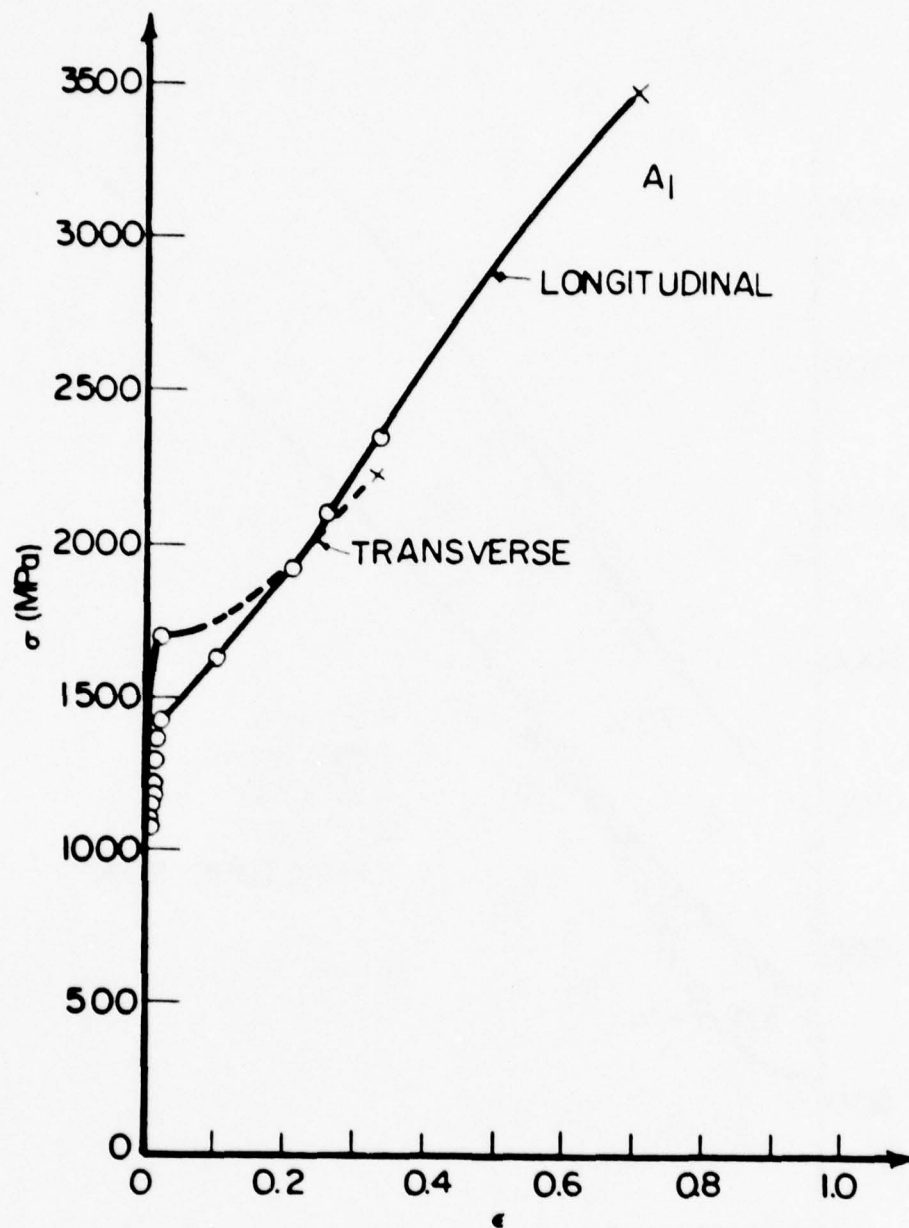
FIG. 18   TRUE STRESS - TRUE STRAIN CURVE OF A1 79% WARM WORKED
TRIP STEEL IN LONGITUDINAL AND TRANSVERSE
DIRECTIONS
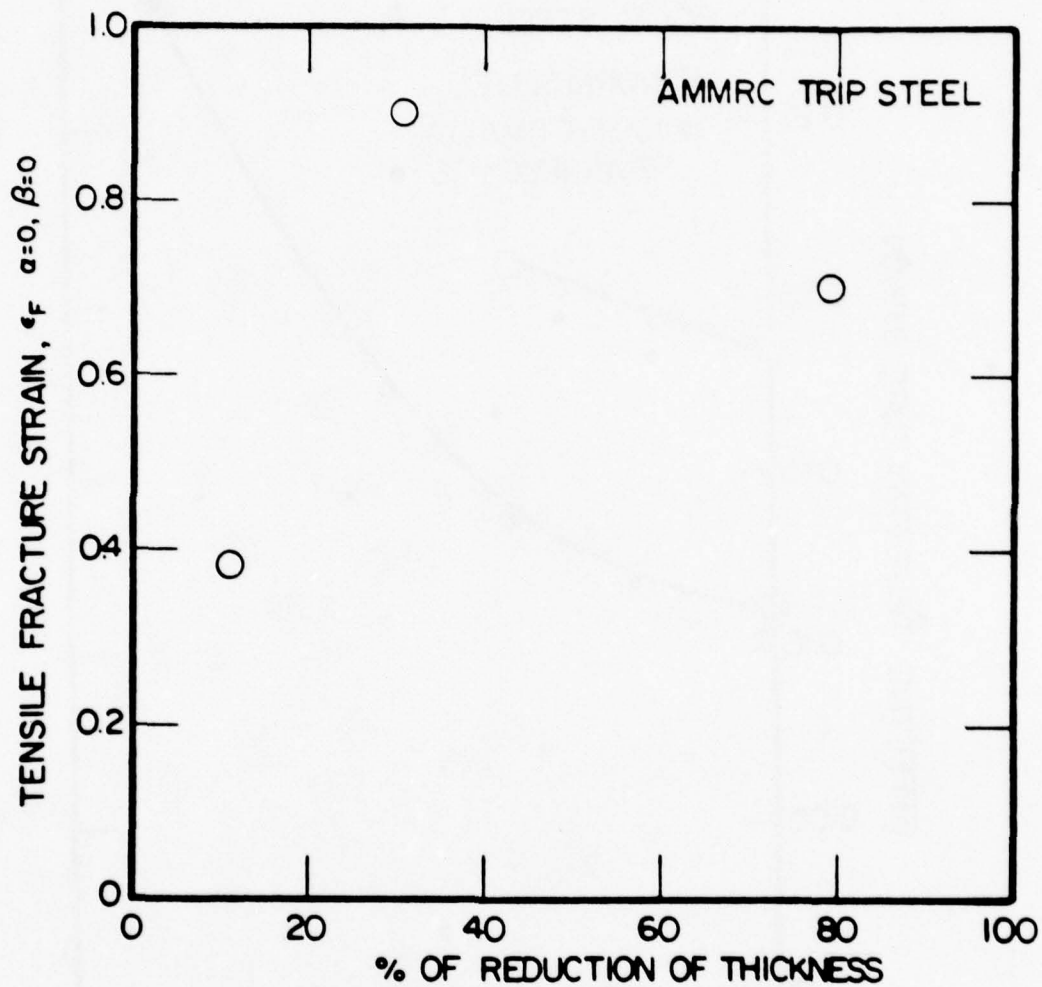
FIG. 19 VALUES OF TENSILE FRACTURE STRAIN OF TRIP STEEL
VS. PERCENT OF REDUTION OF THICKNESS

FIG. 20 EFFECT OF STRAIN RATE ON THE BULGE
DUCTILITY OF 300M STEELS
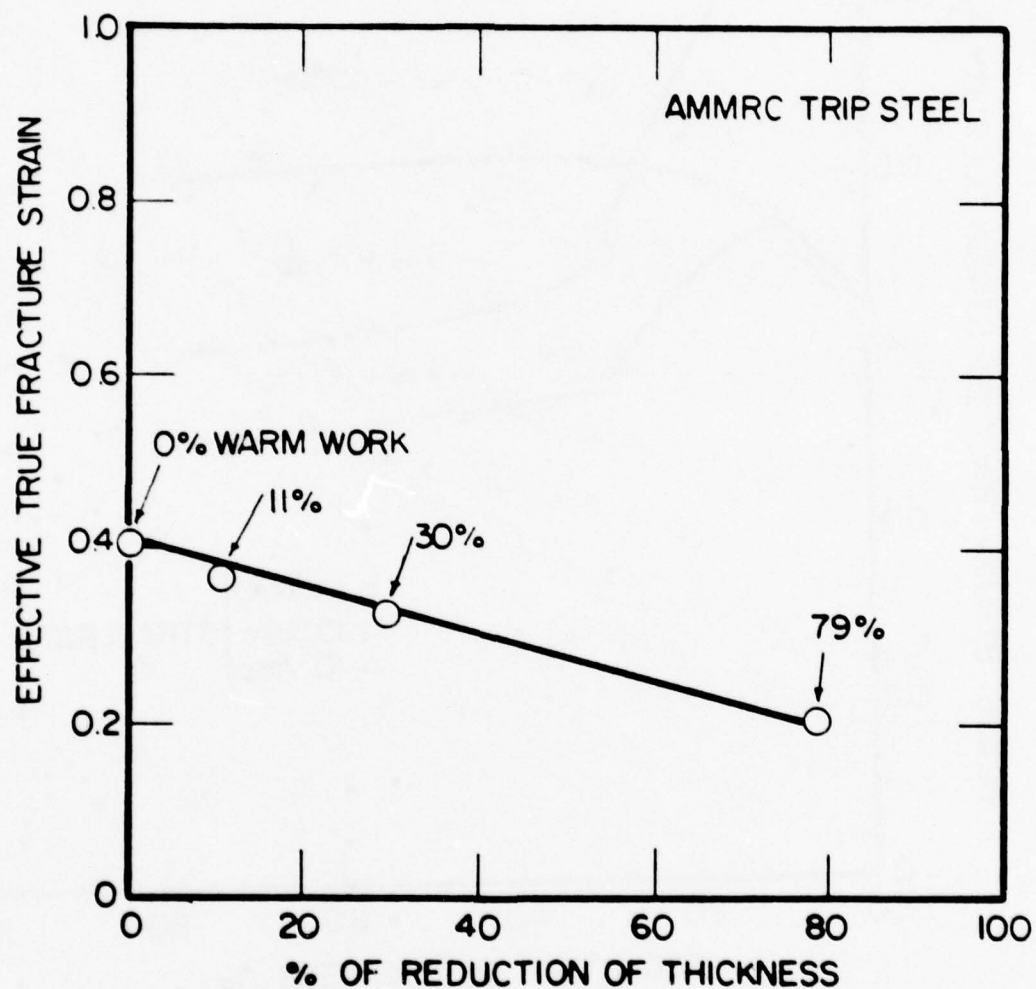
FIG. 21 EFFECT OF THICKNESS REDUCTION BY WARM ROLLING ON THE TRUE FRACTURE STRAIN OBTAINED FROM THE EXPLOSIVE ELLIPTICAL BULGE TEST
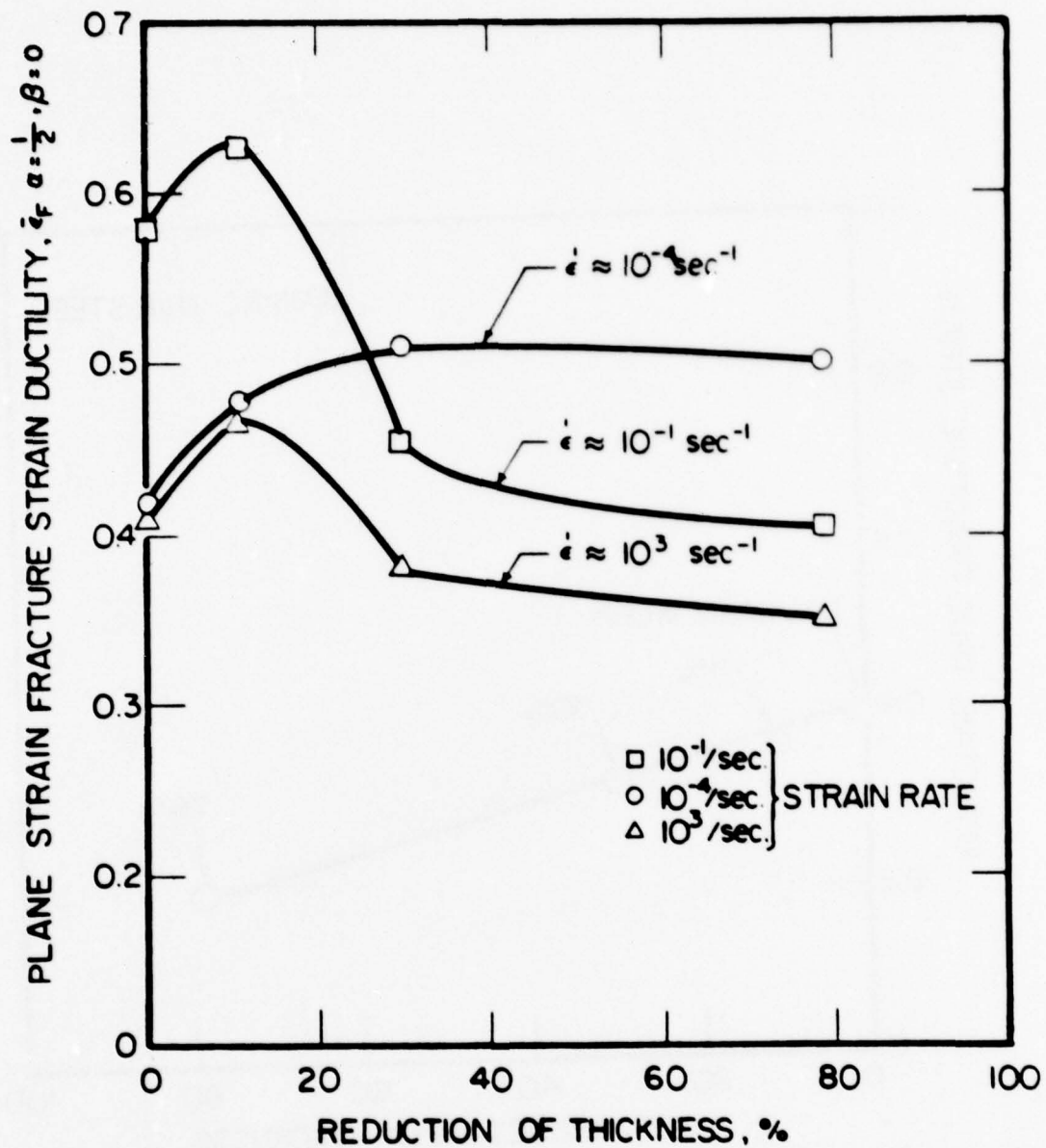
FIG. 22 PLANE STRAIN DUCTILITY VALUES OF TRIP STEEL
VS. PERCENT OF REDUCTION OF THICKNESS AT
THREE STRAIN RATES
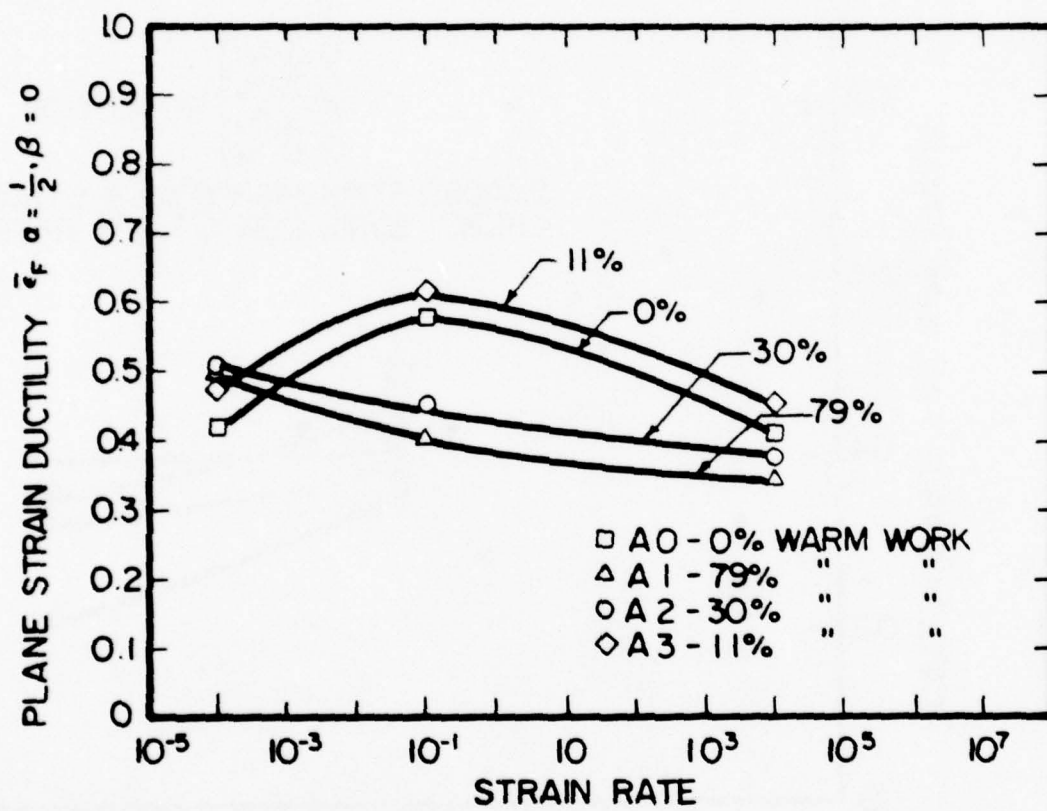
FIG. 23   PLANE STRAIN DUCTILITY VALUES OF TRIP STEELS
VS. STRAIN RATES
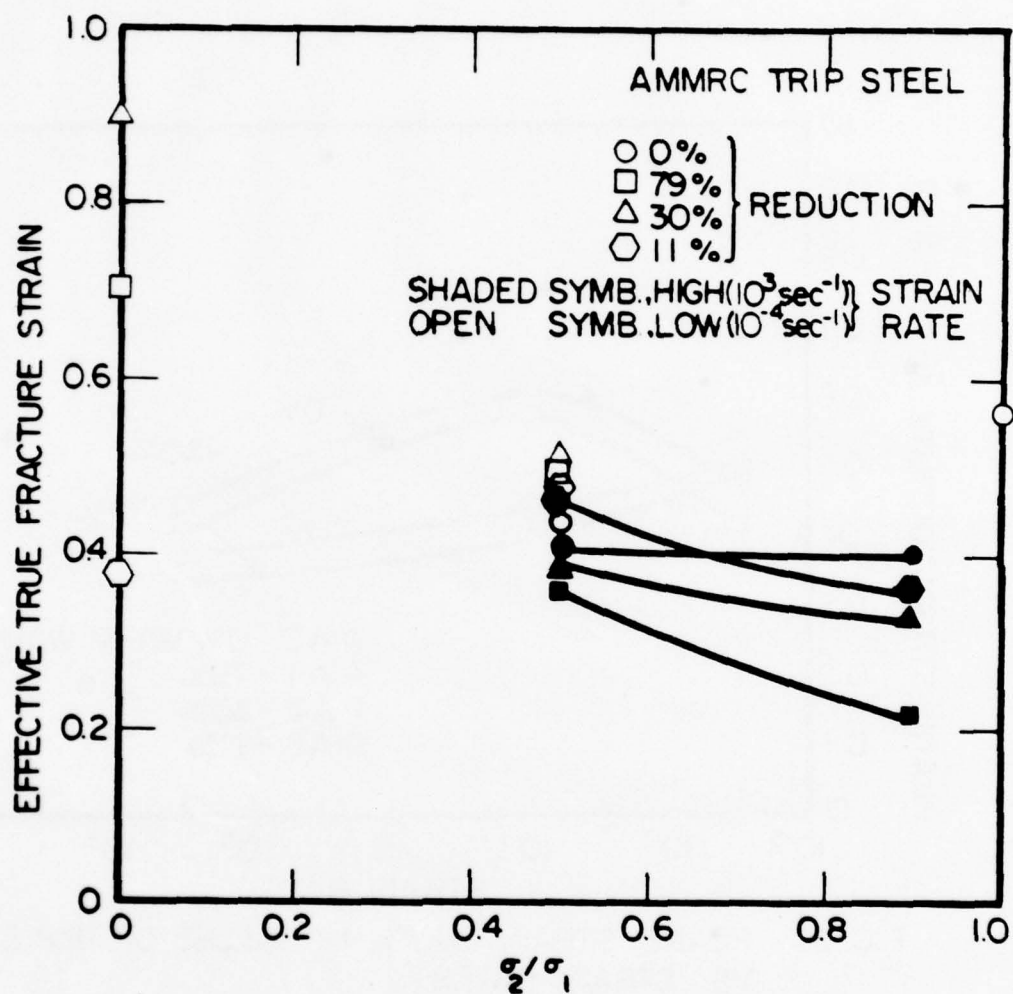
FIG. 24 EFFECT OF STRESS STATE ON THE EFFECTIVE TRUE
FRACTURE STRAIN OF AMMRC TRIP STEEL

TABLE I

CHEMICAL COMPOSITIONS OF
TRIP STEEL AND 300M STEEL

COMPOSITION	300M (Weight Percent)	TRIP (Sheet) (Weight Percent)	TRIP (Plate) (Weight Percent) From Prior Program
C	0.40	0.34	0.27
Mn	0.92	2.12	0.91
Si	1.57	2.06	1.84
Ni	1.90	8.02	8.73
Cr	0.81	8.90	8.81
Mo	0.37	4.14	4.07
P	0.009	0.002	____
S	0.001	0.002	____
N	0.017	____	____
Fe	bal.	bal.	bal.

TABLE II. TESTS CONDUCTED ON 300M AND TRIP STEELS

MATERIAL	1	2	3	4	5	6	7	8	9	10
	Hardness	Tensile		Circular Bulge			Expl. Ellip.Bulge		Plane Strain	
			$(\dot{\varepsilon}{=}10^{-4}\text{sec})$	$(\dot{\varepsilon}{=}10^{-1}\text{sec}^{-1})$	$(\dot{\varepsilon}{=}10^{3}\text{sec}^{-1})$	$(\dot{\varepsilon}{=}10^{-4}\text{sec}^{-1})$	$(\dot{\varepsilon}{=}10^{-1}\text{sec}^{-1})$	$(\dot{\varepsilon}{=}10^{3}\text{sec}^{-1})$		
TRIP STEEL (sheet)										
AO			1	1			1	1	1	1
A1		1	1	1			1	1	1	1
A2			1	1			1	1	1	1
A3			1	2			1	1	1	1
300M										
Normalized		2			1	1				
I. T.			1	2	1	3				
TRIP STEEL (plate)	X					4				

The number in the block indicates the number of tests conducted on that condition.

TABLE III

THE TENSILE PROPERTIES
OF THE 300M STEEL
FOR TWO HEAT-TREATING CONDITIONS

TENSILE PROPERTY	NORMALIZED IN STILL AIR	AUSTENITIZED AT 900°C FOR 30 MIN., I.T. AT 350°C FOR 20 MIN., W.Q.
E	1.50×10^5 MPa	1.76×10^5 MPa
0.2% Yield Strength	_____	1.20×10^3 MPa
Ultimate Tensile Strength	_____	1.79×10^3 MPa
ε_F	0.30	0.23
σ_F	2.92×10^3 MPa	2.16×10^3 MPa
Retained Austenite	6.5%	15.1%

TABLE IV

RESULTS OF TESTS ON TAPERED TENSILE SPECIMENS OF TRIP STEEL

MATERIALS	REDUCTION	FRACTURE STRAIN ε_F	FRACTURE STRESS (MPa) σ_F	E (MPa)
A0	0	_____	_____	1.60×10^5
A1	79%	0.70	3.60×10^3	1.70×10^5
A2	30%	0.90	3.03×10^3	_____
A3	11%	0.37	1.59×10^3	1.46×10^5

TABLE V

THE TENSILE PROPERTIES
OF THE 79% WARM WORKED TRIP STEEL SPECIMENS
IN BOTH THE LONGITUDINAL AND TRANSVERSE DIRECTIONS

	TRANSVERSE DIRECTION	LONGITUDINAL DIRECTION
ε_F	0.34	0.70
σ_F	2.33×10^3 MPa	3.56×10^3 MPa
0.2% Yield Strength	1.45×10^3 MPa	_____
Ultimate Tensile Strength	1.70×10^3 MPa	_____
E	1.70×10^5 MPa	1.70×10^5 MPa

TABLE VI.

RESULTS OF BULGE DUCTILITY OF
300M STEEL AT VARIOUS STRAIN RATES

			Austenitized at 900°C for 30 Min., then isothermally transformed at 350° for 20 min., water quench
Hydraulic	t_o	1.19 mm $\pm$ 0.02 mm	1.22 mm $\pm$ 0.02 mm 1.23 mm
Bulge			
	t_F	0.99 mm $\pm$ 0.02 mm	1.09 mm $\pm$ 0.02 mm 1.10 mm
Testing			
$\dot{\epsilon} \approx 10^{-4}$ sec^{-1}	$\overline{\epsilon}_F$	0.18	0.11 $\underline{0.11}$ Average: 0.11
Hydraulic	t_o	0.51 mm $\pm$ 0.02 mm	0.53 mm $\pm$ 0.02 mm
Press			
	t_F	0.42 mm $\pm$ 0.02 mm	0.46 mm $\pm$ 0.02 mm
Testing			
$\dot{\epsilon} \approx 15^1$ sec^{-1}	$\overline{\epsilon}_F$	0.21	0.14
Dynamic	t_o	————	0.70 mm 0.63 mm $\pm$ 0.01 mm 0.39 mm
Bulge	t_F	————	0.53 mm 0.47 mm $\pm$ 0.01 mm 0.29 mm
Testing		————	
$\dot{\epsilon} \approx 10^3$ sec^{-1}	$\overline{\epsilon}_F$	————	0.28 0.29 $\underline{0.28}$ Average: 0.28

TABLE VII

BULGE TESTING FOR 300M STEEL AND TRIP STEEL

$(\sigma_2/\sigma_1 \; \alpha = 1)$ AT LOW STRAIN RATE $(\dot\varepsilon \approx 10^{-4} \; sec^{-1})$

MATERIAL		INITIAL THICKNESS t_o(mm)	FRACTURE THICKNESS (t_f/mm)	FRACTURE STRAIN $\bar\varepsilon_F$	UNIFORM THICKNESS T_u(mm)	UNIFORM STRAIN ε_u	MAXIMUM PRESSURE (KN)
300M STEEL	Normalized	$1.19 \, {}^{+}_{-} \, 0.02$	$0.99 \, {}^{+}_{-} \, 0.02$	0.18	$1.04 \, {}^{+}_{-} \, 0.02$	0.13	267
	I.T.	$1.22 \, {}^{+}_{-} \, 0.02$	$1.09 \, {}^{+}_{-} \, 0.02$	0.11	$1.12 \, {}^{+}_{-} \, 0.02$	0.09	205
		1.23	1.10	0.11	1.13	0.09	213
TRIP STEEL (SHEET)	0% WW	2.08	1.17	0.58	1.32	0.46	300
	11% WW	$1.60 \, {}^{+}_{-} \, 0.03$	$1.02 \, {}^{+}_{-} \, 0.03$	0.45	$1.12 \, {}^{+}_{-} \, 0.03$	0.36	202
	30% WW	1.56	1.05	0.40	1.17	0.29	231
	79% WW	1.55	1.12	0.32	1.18	0.27	334

TABLE VIII

RESULTS OF EXPLOSIVE ELLIPTICAL BULGE TEST OF TRIP STEEL

MATERIAL % WARM-WORK	t_o^+ mm	t_f^+ mm	$\bar{\varepsilon}_F$
0	0.23	0.15	0.41
79	0.32	0.26	0.21
30	0.67	0.48	0.33
11	0.58	0.41	0.36

+ Thickness values $\pm$ 0.02 mm.

TABLE IX. RESULTS OF PLANE STRAIN TENSILE TEST ON TRIP STEEL AT THREE STRAIN-RATES

STRAIN RATE

$\dot{\varepsilon}$

MATERIAL

% Warm-Work

		0	79	30	11
$10^{-4} sec^{-1}$	t_o (mm)	0.69	0.68	0.63	0.56
	t_f (mm)	0.48	0.44	0.405	0.37
	$\bar{\varepsilon}_F = \frac{2}{\sqrt{3}} \ln \frac{t_o}{t_f}$	0.42	0.50	0.51	0.48
$10^{-1} sec^{-1}$	t_o (mm)	0.71	0.61	0.53	0.60
	t_f (mm)	0.43	0.43	0.36	0.35
	$\bar{\varepsilon}_F = \frac{2}{\sqrt{3}} \ln \frac{t_o}{t_f}$	0.58	0.40	0.45	0.63
$10^{3} sec^{-1}$	t_o (mm)	0.70	0.61	0.61	0.61
	t_f (mm)	0.49	0.45	0.44	0.41
	$\bar{\varepsilon}_F = \frac{2}{\sqrt{3}} \ln \frac{t_o}{t_f}$	0.41	0.35	0.38	0.47

TABLE X

THE AMOUNT OF MARTENSITE FORMED NEAR THE FRACTURE SURFACE

OF THE PLANE STRAIN SPECIMENS OF TRIP STEEL ($\alpha = \sigma_2/\sigma_1 = 1/2$)

% WARM-WORK / STRAIN RATE	0	79	30	11
$\dot{\varepsilon} = 10^{-4}$ sec^{-1}	14.0%	>20%	>20%	>20%
$\dot{\varepsilon} = 10^{-1}$ sec^{-1}	19.0%	9.0%	12.0%	>20%
$\dot{\varepsilon} \approx 10^{3}$ sec^{-1}	5.0%	4.0%	1.0%	3.0%

REFERENCES

1. Zackay, V.F., Parker, E.R., Fahr, D. and Busch, R., "The Enhancement of Ductility in High-Strength Steels", Trans. ASM, Vol. 60, P. 252. (June 1967).

2. Weiss, V., "Transformation Plasticity", ASM Pre-Congress Seminar on the "Inhomogeneity of Plastic Deformation"; Detroit. Chapter 6, P. 135 (October 1971).

3. Antolovich, S.D. and Singh, B., "Observations of Martensite Transformation and Fracture in TRIP Steel", Metallurgical Trans., Vol. I, No. 12, P. 3463 (December 1970).

4. Weiss, V., Schroder, K., Sanford, W., Chandan, H., Kunio, T., Lal, D, and Sengupta, M., "The Relationships Between the Transformation Characteristics and the Fracture and Fatigue Properties of TRIP Steels", Final Report, AMMRC CTR 73-50 (December 1973).

5. Weiss, V., Schroder, K., Sherman, P. and Pan, A., "The Relationships Between the Transformation Characteristics and the Fracture and Fatigue Properties of TRIP Steels and Other Metastable Austenite Steels", Final Report, AMMRC CTR 77-1 (January 1977).

6. Gold, E. and Koppenaal, T.J., "Anomalous Ductility of TRIP Steel", Trans. ASM, Vol. 62, P. 607 (1969).

7. Azrin, M., Olson, G.B., and Gagne, R.A., "Inhomogeneous Deformation and Strain-Rate Effects in High Strength TRIP Steels", AMMRC TR 73-12 (March 1973).

8. Weiss, V., Kasai, Y., Liu, K., Sanford W., and Sieradski, K. "The Significance of Material Ductility to the Reliability and Load Carrying Capacity of Peak Performance Structures", Syracuse University Final Report to NASC, No. N00019-75-C-0065 (December 1975).

9. Weiss, V., Sengupta, M., and Sanford, W., "The Significance of Materials Ductility to the Reliability and Load Carrying Capacity of Peak Performance Structures (U)", Syracuse University Final Report to NASC, No. MS-VW-1708-F674 (June 1974).

10. Weiss, V. and Sengupta, M., "Correlation Between Fracture Toughness and Material Ductility", Proc. Third Int. Conf. on Frac., Munich, Germany (1973).

11. Corrigan, D.A., Travis, R.E., Ardito, V.P., and Adams, C.M., Jr. "Biaxial Strengths of Welds in Heat Treated Steel Sheet", Welding Research Supplement, Vol. 4, p. 123 (March 1962)

12. Durnin, J. and Ridal, K.A., "Determination of Retained Austenite in Steel by X-ray Diffraction", J. Iron Steel Inst., Vol. 207, p. 60 (January 1968).

13. Lin, H.H., "Deformation Characteristics of Face-Centered Cubic and Hexagonal Metals and Alloy", Ph.D. Dissertation, Syracuse University (November 1972).

14. Biegel, J.E., Private Communication (1975).

15. Mendelson, A., "Plasticity: Theory and Application". 2nd. Edition, MacMillan Company, New York (1968)

16. Beeuwkes, R. Jr., Chait, R., and Lin, H.H., "Indentation Hardness as a Means for Determining Uniaxial Flow Curves", Presented in International Symposium on the Science of Hardness-Testing and Its Application, Detroit, Michigan (October 1971).

17. Bressanelli, J.P. and Moskowitz, A., "Effects of Strain Rate, Temperature and Composition on Tensile Properties of Metastable Austenitic Stainless Steels", Trans. ASM, Vol. 59, p. 223 (1966).

18. Watson, J.F. and Christian, J.L., "A Study of Austenite Decomposition at Cyogenic Temperature", General Dynamics Astronautics 3rd Quarterly Report to USAFAS. No. AF 33(616)-7984 (ERR-An-057) December, 1962.

19. Greenberg, S., American Instrument Company, Private Communication. (February 1973).

20. Larson, F., AMMRC, Private Communication.

21. Weiss, V., "Material Ductility and Fracture Toughness of Metals", Proceeding of the International Conference on Mechanical Behavior of Materials, Kyoto, Japan, Vol. I, p. 1098 (1972)

Army Materials and Mechanics Research Center
Watertown, Massachusetts 02171
EXPLORATORY STUDY OF THE DYNAMIC
FRACTURE DUCTILITY OF TRIP AND
300M STEELS-Volker Weiss, Albert
Wu, and John Biegel, Department
of Chemical Engineering and Materials Science, Syracuse University, Syracuse, N.Y. 13210

Technical Report AMMRC TR 79-8, February, 1979,
16 pp-ill-tables, Contract DAAG46-77-0018
D/A Project: 1L162105AH84

AD
UNCLASSIFIED
UNLIMITED DISTRIBUTION

Key Words
TRIP steels
300M steels
High strength steels
Mechanical properties
Dynamic properties
Transformation plasticity
Fracture

The bulge characteristics of 300M steel and TRIP steel were studied at various strain rates and stress states. The 300M steel was heat-treated to two conditions: isothermally transformed and normalized. The TRIP steel was processed to four conditions by means of various amounts of warm working. The inherent directionality of TRIP steel required the development of a biaxial test for various strain rates other than the equibiaxial bulge test where the stress ratio, $\alpha = \sigma_2/\sigma_1$ is not equal to 1. Two testing methods were developed: 1) a bulge test through an elliptical die, which gives a stress state $\alpha = 0.5$, and 2) a plane strain tensile test, which gives a stress state of $\alpha = 1/2$.

The basic mechanical properties of the materials are given through their true strain [ϵ], true stress [σ] strain curves. The equibiaxial bulge tests at three strain rates ($\dot{\epsilon} = 10^{-3}$ sec^{-1}, 10^{-1} sec^{-1} on the isothermally transformed 300M steel show that the fracture ductility increases with increasing strain rate. On the basis of the reported correlation between a true effective fracture strain from a bulge test and the plane strain fracture toughness, a similar increase in fracture toughness with increasing strain rate is expected. At low strain rate the fracture ductility of TRIP steel is a function of the stress state at fracture and of the amount of warm-work during TRIP processing. The minimum value of the fracture ductility of TRIP steel at low strain rates is observed for a stress state $\alpha = 1$, which is in agreement with previous results on high strength steel and the critical mean stress fracture criterion proposed by Weiss. For the two high strength TRIP steels (7% warm-work and 30% warm-work), the plane strain fracture ductility decreases with increasing strain rate. A similar decrease of the plane strain fracture toughness with increasing strain rate is expected. Adiabatic heating and consequent repression of the martensite formation is suggested as the principal responsible mechanism.

DISTRIBUTION LIST

No. of Copies	To
1	Office of the Under Secretary of Defense for Research and Engineering, The Pentagon, Washington, D. C. 20301
12	Commander, Defense Documentation Center, Cameron Station, Building 5, 5010 Duke Street, Alexandria, Virginia 22314
1	Metals and Ceramics Information Center, Battelle Columbus Laboratories, 505 King Avenue, Columbus, Ohio 43201

Deputy Chief of Staff, Research, Development, and Acquisition, Headquarters, Department of the Army, Washington, D. C. 20310
1 ATTN: DAMA-ARZ

Commander, Army Research Office, P. O. Box 12211, Research Triangle Park, North Carolina 27709
1 ATTN: Information Processing Office

Commander, U. S. Army Materiel Development and Readiness Command, 5001 Eisenhower Avenue, Alexandria, Virginia 22333
1 ATTN: DRCLDC, Mr. R. Zentner

Commander, U. S. Army Materiel Systems Analysis Activity, Aberdeen Proving Ground, Maryland 21005
1 ATTN: DRXSY-MP

Commander, U. S. Army Missile Research and Development Command, Redstone Arsenal, Alabama 35809
1 ATTN: DRDMI-RKK, Mr. C. Martens, Bldg. 7120
1   Technical Library

Commander, U. S. Army Armament Research and Development Command, Dover, New Jersey 07801
2 ATTN: Technical Library
1   DRDAR-SCM, J. D. Corrie
1   DRDAR-QAC-E

Commander, U. S. Army Natick Research and Development Command, Natick, Massachusetts 01760
1 ATTN: Technical Library

Commander, U. S. Army Tank-Automotive Research and Development Command, Warren, Michigan 48090
1 ATTN: DRDTA-RKA
2   DRDTA-UL, Technical Library

No. of Copies	To

Commander, White Sands Missile Range, New Mexico 88002
1 ATTN: STEWS-WS-VT

Director, U. S. Army Ballistic Research Laboratory,
Aberdeen Proving Ground, Maryland 21005
1 ATTN: DRDAR-TSB-S (STINFO)

Commander, Dugway Proving Ground, Dugway, Utah 84022
1 ATTN: Technical Library, Technical Information Division

Commander, Harry Diamond Laboratories, 2800 Powder Mill Road,
Adelphi, Maryland 20783
1 ATTN: Technical Information Office

Commander, Picatinny Arsenal, Dover, New Jersey 07801
1 ATTN: SARPA-RT-S

Commander, Redstone Scientific Information Center, U. S. Army Missile
Command, Redstone Arsenal, Alabama 35809
4 ATTN: DRDMI-TB

Chief, Benet Weapons Laboratory, LCWSL, USA ARRADCOM, Watervliet,
New York 12189
1 ATTN: DRDAR-LCB-TL

Commander, U. S. Army Foreign Science and Technology Center,
220 7th Street, N. E., Charlottesville, Virginia 22901
1 ATTN: Military Tech, Mr. Marley

Director, Eustis Directorate, U. S. Army Air Mobility Research and
Development Laboratory, Fort Eustis, Virginia 23604
1 ATTN: Mr. J. Robinson, DAVDL-E-MOS (AVRADCOM)

Commander, U. S. Army Engineer School, Fort Belvoir, Virginia 22060
1 ATTN: Library

Naval Research Laboratory, Washington, D. C. 20375
1 ATTN: Dr. J. M. Krafft - Code 8430
2   Dr. G. R. Yoder - Code 6384

Chief of Naval Research, Arlington, Virginia 22217
1 ATTN: Code 471

Air Force Materials Laboratory, Wright-Patterson Air Force Base, Ohio 45433
2 ATTN: AFML/MXE/E. Morrissey
1   AFML/LC
1   AFML/LLP/D. M. Forney, Jr.
1   AFML/MBC/Mr. Stanley Schulman

No. of Copies	To

National Aeronautics and Space Administration, Washington, D. C. 20546
1 ATTN: Mr. B. G. Achhammer
1   Mr. G. C. Deutsch - Code RW

National Aeronautics and Space Administration, Marshall Space Flight
Center, Huntsville, Alabama 35812
1 ATTN: R. J. Schwinghammer, EH01, Dir, M&P Lab
1   Mr. W. A. Wilson, EH41, Bldg. 4612

1 Librarian, Materials Sciences Corporation, Blue Bell Campus, Merion Towle
   House, Blue Bell, Pennsylvania 19422

Panametrics, 221 Crescent Street, Waltham, Massachusetts 02154
1 ATTN: Mr. K. A. Fowler

Wyman-Gordon Company, Worcester, Massachusetts 01601
1 ATTN: Technical Library

Lockheed-Georgia Company, 86 South Cobb Drive, Marietta, Georgia 30063
1 ATTN: Materials and Processes Engineering Dept. 71-11, Zone 54

General Dynamics, Convair Aerospace Division, P.O. Box 748,
Fort Worth, Texas 76101
1 ATTN: Mfg. Engineering Technical Library

1 Mechanical Properties Data Center, Belfour Stulen Inc.,
   13917 W. Bay Shore Drive, Traverse City, Michigan 49684

Director, Army Materials and Mechanics Research Center,
Watertown, Massachusetts 02172
2 ATTN: DRXMR-PL
1   DRXMR-P
2   DRXMR-PR
1   DRXMR-AP
1   DRXMR-L
1   DRXMR-E
1   DRXMR-EM
5   DRXMR-EM, Dr. Azrin